U.S. FOREST SERVICE
RESEARCH PAPER INT-25, 1966

AD 647136

AVAILABILITY NOTICE

Distribution of this document is unlimited

PROJECT FIRE SCAN
FIRE DETECTION INTERIM REPORT

April 1962 to December 1964 (Work Unit 2521A)

ARCHIVE COPY

D D C
FEB 23 1967

U.S. Department of Agriculture — Forest Service
Intermountain Forest and Range Experiment Station
Northern Forest Fire Laboratory
Missoula, Montana

ACCESSION for
CFSTI WHITE SECTION
DDC BUFF SECTION
UNANNOUNCED
JUSTIFICATION
BY
DISTRIBUTION/AVAILABILITY CODES
DIST. AVAIL. and/or SPECIAL

ACKNOWLEDGMENT

The authors gratefully acknowledge financial, technical, and cooperative assistance by several agencies and organizations in accomplishing the tasks included in this report. Among them are:

- Department of the Army, Office of the Secretary of the Army
- Department of Defense, Advanced Research Projects Agency
- Infrared Physics Laboratory, Institute of Science and Technology, University of Michigan
- HRB-Singer, Incorporated
- State of Montana, Forestry Department
- Texas Instrument Company
- U.S. Forest Service National Forest Administration
- The Electronic Command, U.S. Army Materiel Command

Headquarters for the Intermountain Forest and Range Experiment Station are in Ogden, Utah. Project headquarters are also at:

Boise, Idaho

Bozeman, Montana (in cooperation with Montana State University)

Logan, Utah (in cooperation with Utah State University)

Missoula, Montana (in cooperation with University of Montana)

Moscow, Idaho (in cooperation with the University of Idaho)

Provo, Utah (in cooperation with Brigham Young University)

U.S. FOREST SERVICE
RESEARCH PAPER INT-25, 1966

PROJECT FIRE SCAN
FIRE DETECTION INTERIM REPORT

April 1962 to December 1964

by
Ralph A. Wilson, Physicist
and
Nonan V. Noste, Research Forester

THE EVALUATION OF AN AIRBORNE INFRARED MAPPER
AS A TOOL FOR DETECTING AND MEASURING FIRES
(Work Unit 2521A)

for
Department of Defense, Office of Civil Defense
Contract OCD-OS-62-174
and
Department of Defense, Advanced Research Projects Agency
ARPA Order No. 636, Program Code No. 5860

OCD REVIEW NOTICE

This report has been reviewed in the Office of Civil Defense and approved for publication. Approval does not signify that the contents necessarily reflect the views and policies of the Office of Civil Defense.

INTERMOUNTAIN FOREST AND RANGE EXPERIMENT STATION
U.S. DEPARTMENT OF AGRICULTURE — FOREST SERVICE
NORTHERN FOREST FIRE LABORATORY
MISSOULA, MONTANA

AVAILABILITY NOTICE. — Distribution of this document is unlimited.

CONTENTS

	Page
INTRODUCTION	2
PHASE I TEST PROGRAM	3
INTRODUCTION	3
EQUIPMENT	3
DEVELOPMENT OF TEST PROCEDURE	3
DISCUSSION OF RESULTS	5
SUMMARY, PHASE I	7
PHASE II TEST PROGRAM	7
INTRODUCTION	7
DEVELOPMENT OF EQUIPMENT	7
TEST PROCEDURE	8
DISCUSSION OF RESULTS	10
SUMMARY, PHASE II	15
PHASE III TEST PROGRAM	16
OBJECTIVES	16
FIRE DETECTION TESTS	16
FIRE PATROL	17
Equipment and Test Procedures	17
Patrol Area	17
Patrol Flight	17
MOUNTAINTOP TESTS	17
General Discussion	17
Preparation of Program	18
Instrumentation	19
Discussion of Tests at 45° Plot	24
Detection Predictions at 45° for Spot Fire Models	28
Detection Probability Beyond 45°	30
Summary of Mountaintop Test Series	35
CONCLUSION	36
SUMMARY OF PHASES I, II, and III	36
PLANS FOR THE FUTURE	36
APPENDIX I — DESCRIPTION OF TEST AREA	38
APPENDIX II — CRITERIA FOR SPECTRAL RESPONSIVITY	42
APPENDIX III — SENSITIVITY OF SCANNING SYSTEM	44
APPENDIX IV — CRITERIA FOR DETECTION	46
APPENDIX V — ATTENUATION OF RADIATION	50

ILLUSTRATIONS

Figure		*Page*
1	Percent transmission versus vertical angle for four coniferous species.	5
2	Percent total detection versus vertical angle for three timber stands.	6
3	Percent total detection versus basal area classed for three altitudes and two system resolutions.	6
4	Equipment modification: *A*, Infrared receiver modified to a 10-inch focal length system; *B*, Polaroid image recording camera.	8
5	Fire array target pattern.	10
6	Samples of flight test imagery: *A*, Imagery obtained with scanner tilted at 20°; *B*, imagery with scanner tilted at 50°.	11
7	Detection probability as a function of vertical angle and fire radius for lodgepole pine test area.	12
8	Detection probability as a function of vertical angle and fire radius for ponderosa pine test area.	12
9	Detection probability as a function of vertical angle and fire radius for larch—Douglas-fir test area.	12
10	Detection probability as a function of vertical angle and fire radius for Engelmann spruce—alpine fir test area.	12
11	Accumulative detection probability versus vertical angle and fire size for lodgepole pine test area.	14
12	Accumulative detection probability versus vertical angle and fire size for ponderosa pine test area.	14
13	Accumulative detection probability versus vertical angle and fire size for larch—Douglas-fir test area.	14
14	Accumulative detection probability versus vertical angle and fire size for Engelmann spruce—alpine fir test area.	14
15	Mountaintop scanner installation.	18
16	Test area from scanner location.	18
17	Bear Creek test site map.	19
18	Block diagram of mountaintop scanner instrumentation.	20
19	Polaroid photographs of oscilloscope readout: *A* (1825 hours, 10/13) and *B* (0012 hours, 10/14), Change in background signal level over a 5-3/4-hour period; *C* and *D* (1/16-square-foot target), full scan sweep on *C*, sweep expanded and delayed for more precise signal observation on *D*.	21
20	Polaroid photographs of oscilloscope readout: *A*, Target (35,75) signal and system noise with no electronic filter; *B*, same sweep with 150 kc. low-pass electronic filtering; *C*, measurement of scanner resolution, two fires 1.7 milliradians apart; *D*, measurement of scanner resolution, two fires 2.6 milliradians apart.	22

Figure		Page
21	*A*, Instrument calibration curve; *B*, calibration curve showing nonlinear response of the voltage gain amplifier.	23
22	Plan view of individual tree boles and crowns within the 45° test area.	23
23	Signal voltage profile of 45° test area, from 1-square-foot charcoal sources.	24
24	*A*, Accumulative percent of total observations versus signal strengths for 1-, 2-, 3-, and 5-square-foot targets; *B*, frequency of occurrence of equivalent unobscured source sizes (1-square-foot targets at 45°).	25
25	Photograph of general canopy character of 45° plot from evenly spaced plot locations. Numbers in parentheses refer to plot location abscissa and ordinate associated with figures 22 and 23.	26
26	Photograph of selected plot locations showing canopy characteristics associated with several values of signal strength.	27
27	Measured percent of positive detections as a function of increasing test plot size.	28
28	Percent detection at 45° determined for three fire models as a function of model size and signal threshold.	29
29	Frequency distribution of distances from random locations to nearest positive detection.	30
30	Frequency distribution of signal strengths versus size of the solid fire model A.	31
31	Percent detection versus aspect angle for several detection signal thresholds.	32
32	Phase II, larch—Douglas-fir flight data to 50° extended past 60° by the mountaintop test data.	33
33	Frequency of occurrence for all 5-square-foot target arrays, 45° to 69°, by signal strength.	33
34	Absolute spectral emissive powers for black bodies at various temperatures.	43
35	Aircraft scanning geometry.	47
36	Typical video signal oscilloscope trace.	47
37	Pulse-height discrimination circuit separating low amplitude, high frequency signal from background.	48
38	Lower limit values of (target area)/(aircraft altitude)^2 ratio as function of peak-to-peak background temperature variation for several target temperatures, assuming detection criteria of Eqn. 7 in the text.	49
39	Spectral characteristics of a typical detector and filter.	51
40	Typical atmospheric transmission curve; 16.25 km. sea level path, 68.7° F., 53-percent relative humidity, 15.1 cm. H_2O in path.	51

Figure		*Page*
41	Spectral transmission of water for various optical paths.	52
42	Spectral transmission of CO_2 for various optical paths.	52
43	Variation in atmospheric CO_2 concentration with altitude normalized to sea level.	53
44	Precipitable H_2O concentration as a function of atmospheric temperature and relative humidity.	53
45	Percent transmission of water in the 2.8- to 5.8-micron band versus concentration of precipitable water.	54
46	Observed and predicted obscurations from a tree bole model.	54

PROJECT FIRE SCAN

INTERIM REPORT

April 1962 to December 1964

This work was accomplished under Work Order OCD-OS-62-174. This agreement outlined a three-phase test program to evaluate airborne infrared devices as tools for use in fire control. After Phase II was completed, the tasks were more specifically defined. At that time the program was administratively divided into its two natural components — fire mapping and fire detection.

This report summarizes the fire detection work from April 1962 to December 1964. The fire mapping effort will be discussed in a later report.

INTRODUCTION

The original program objectives were to develop and test a heat-sensitive system capable of: (1) locating small fires, (2) mapping fire perimeters, and (3) measuring rates of fire spread. The usefulness of infrared mappers was to be examined by surveillance of fire sources in forest environments. The capability for locating fire perimeter and detecting incipient fires was to be compared with that of aerial patrol and methods of ground observation now in use.

The work agreement outlined a three-phase test program. After Phase II was completed, the tasks were more specifically defined and the program was divided into its two natural components — fire mapping and fire detection. This separation allowed both programs to concentrate on development of systems specifically adapted to their unique problems. The goal of the detection program is to develop the capability for precisely locating small fire targets over extended land areas.

PHASE I TEST PROGRAM

INTRODUCTION

Preliminary work included acquiring the necessary instrumentation and familiarizing project personnel with the equipment and test procedures. The infrared instrumentation used during the period covered by this report was designed and built for other uses, and hence required considerable modification for use in fire surveillance.

EQUIPMENT

The scanner system used during this phase of the program consisted of a receiver unit and control-readout console. The infrared optical-mechanical receiver was installed in the nose hatch of a modified Beechcraft AT-11 aircraft. The optical receiver scanned an 80°-wide field (40° to either side of vertical in normal operation) perpendicular to the aircraft's line of flight. Continuous-strip photographic recordings of the cathode ray tube (C.R.T.) readout gave map-like imagery of the terrain's thermal detail. The optical resolution at this time was approximately 4 milliradians. The scanning geometry was similar to that discussed in Appendix IV.

The receiver unit could be rotated into a "side-looking" mode, i.e., from the vertical to 80° on one side of the flight path. This modification was necessary in order to examine the feasibility of wider flight paths.

The control-readout console was mounted in the passenger cabin of the aircraft. Monitors included C.R.T. presentations of the raw video signal ("A"-scan) and an auxiliary TV-like raster scan of the thermal imagery ("B"-scan). Controls adjusted the video signal on the C.R.T. readout for proper photographic exposure and aircraft flight parameters. Electronic "gain" and "level" adjustments controlled the photographic contrast and film density, respectively. A V/H (Velocity/Height) control of the strip film drive speed provided imagery of minimum distortion (see Appendixes III and IV).

Control settings were not optimized prior to or during the test flights. The test imagery was unobservable until the film had been returned to the Laboratory and developed. These recording limitations seriously hampered evaluation of the test results that were directly dependent upon the imagery.

Five types of detectors and optical filters of six different spectral bands were obtained with the scanning equipment. The detector-filter combinations used during the fire detection tests were chosen by subjective evaluation of image quality.

DEVELOPMENT OF TEST PROCEDURE

Instrumented aircraft flew tests over forested test plots that contained artificial fire targets. Very little was known about the specific radiation characteristics of fires burning under marginal conditions. A heat source of arbitrary size and temperature simulated an incipient forest fire. The target had to be uniform, repeatable, portable, and safe to use in a forest environment during high fire-danger periods. A 14-inch-diameter bucket, 9 inches deep, partially filled with sand, then filled to the brim with 10 pounds of charcoal, was selected as the standard target. Burning charcoal temperatures, measured with a thermocouple, ranged from 700° F. to 1,190° F., and averaged 892° F. A radiometer measurement of 895° F. (effective radiometric temperature) agreed closely.

A time-history record showed the source emission to be steady between one-half hour and 5 hours after ignition. Variation of radiant energy, measured as a function of vertical angle and plotted as a cosine function, showed that this source closely approximates a Lambertian radiator. These targets have proved quite satisfactory and have been used through-

out the program, although at times sparks from them are a fire hazard.

The first night and day flights were conducted over a relatively flat, barren target area adjacent to Missoula, Montana. The operators were familiarized with equipment, and the several detector-filter combinations were examined. Unfiltered indium antimonide, lead sulfide, and lead telluride detectors were used in combination with a 3-micron, long-pass filter. Initial tests showed the lead sulfide detectors[1] with a 3.4- to 4.1-micron filter gave the best imagery during the daytime tests; however, these results were not acceptable. Subsequent searching for a suitable daytime detector-filter combination showed that an indium antimonide detector and a 4.5- to 5.5-micron filter were the best available, but daytime results were still marginal.

For best results at night no filter was used. Little difference was apparent between lead sulfide and indium antimonide detectors. The detection tests that followed utilized both lead sulfide and indium antimonide detectors for night operation, and indium antimonide with a 4.5- to 5.5-micron filter during daytime conditions.

Measurements made by the Materiel Branch, Electronic Research Development Laboratory, Fort Belvoir, Va.,[2] showed that coniferous foliage and tree bark are opaque to energy radiated in the infrared portion of the spectrum. However, no data were available concerning the obscuration of small fires by a forest canopy. The distribution, size, shape, and total number of transmission paths through a canopy were likely to vary with forest type, site quality, age, stand density, and other factors that affect stand morphology.

A major objective of the program was to determine the effect of timber cover on detection probability. Another was to develop a stand measurement to predict the obscuration effect of the various timber stands. An optimum vertical angle, within 20° of the zenith, was anticipated at which the canopy would least interfere with detection. A maximum angle beyond which detection would be virtually impossible was also predicted.

Only four coniferous species were considered initially — lodgepole pine (*Pinus contorta* Dougl.), ponderosa pine (*Pinus ponderosa* Laws.), Douglas-fir (*Pseudotsuga menziesii* var. *glauca* (Beissn.) Franco), and Engelmann spruce (*Picea engelmannii* Parry). These species were selected on the basis of shade tolerance. Tolerance[3] is an expression of a species' ability to endure shade. Thus, tolerance is a good guide to canopy density since species that require less light are more likely to develop very dense canopy covers. The species selected sampled the range of canopy densities found in western Montana.

Four timbered areas were selected to test the effect of timber cover on detection probability. Flight tests provided data on three types of forest cover — ponderosa pine, Douglas-fir, and Engelmann spruce. Relatively pure, but nonhomogeneous, stands were selected to provide a large variation in stand form, stand density, and canopy characteristics. For example, the ponderosa pine test area contained units of open grown, overmature, thrifty mature, and small stagnated trees.

Also considered in selecting test areas were: (1) recognizable terrain features to facilitate navigation, (2) peaks and ridges that make night air operations hazardous, (3) level topography within the area, and (4) distance from Missoula.

Twenty plot centers in a 4 by 5 pattern were systematically located 500 feet apart throughout each test area. Each plot was described according to slope, aspect, and basal area within a variable radius (Bitterlich[4])

[1] *Identification of the lead sulfide detector must be questioned by the sensitivity parameters required for this performance. The best PbS detectors now available have peak responses at 3.2μ and time constants of greater than 1 msec. (for optimum responses, less than 5μ sec. is required). This identification was made by printed labels on borrowed equipment.*

[2] *Unpublished report.*

[3] *Baker, Frederick S. A revised tolerance table. J. Forest. 47: 179-181. 1949.*

[4] *Grosenbaugh, L. R. Plotless timber estimates — new, fast, easy. J. Forest. 50: 32-37. 1952.*

plot. Total height, percent of live crown, crown diameter, diameter at breast height (d.b.h.), and species were recorded for each tree within the plot, and two timber crown photographs were taken from each plot center. This description aided the qualitative analysis of the flight data.

At three plots within each test area a theodolite measured the portion of the hemisphere over the plot center covered by forest vegetation. The theodolite was mounted on a standard tripod, and leveled. The telescope was pointed toward the zenith (90°) and the observer would estimate the percent of the 2° field of view filled by boles and foliage. The percent of open canopy was estimated at each 2° interval, from 90° down to 20° above the horizon. The telescope was again pointed toward the zenith, the azimuth lock released, and the theodolite rotated to another random azimuth angle.

This procedure was repeated eight times at each plot. Figure 1 is a plot of the curves generated by averaging the eight readings for each vertical angle. The curves show no tendency to peak below the zenith (0°). Although they are not well defined, the transmission curves decline steadily toward the horizon. Ponderosa pine and Douglas-fir are similar, with the Engelmann spruce significantly more dense.

Data acquisition flights were coordinated between the aircraft crew and ground crew. The ground crew ignited the 20 charcoal fires at least 30 minutes prior to the time the aircraft was scheduled over the area. The aircrew consisted of a pilot and one operator; occasionally a third member acted as observer and relief operator. Passes were flown from altitudes of 2,000 feet to 10,000 feet over terrain. Courses were charted to position the aircraft directly over the test area and to place all targets within the field of view of the scanner at the proper vertical aspect angles.

DISCUSSION OF RESULTS

Aircraft navigation over the test area (dependent upon the map presentation of a 5-inch monitor scope) was not satisfactory

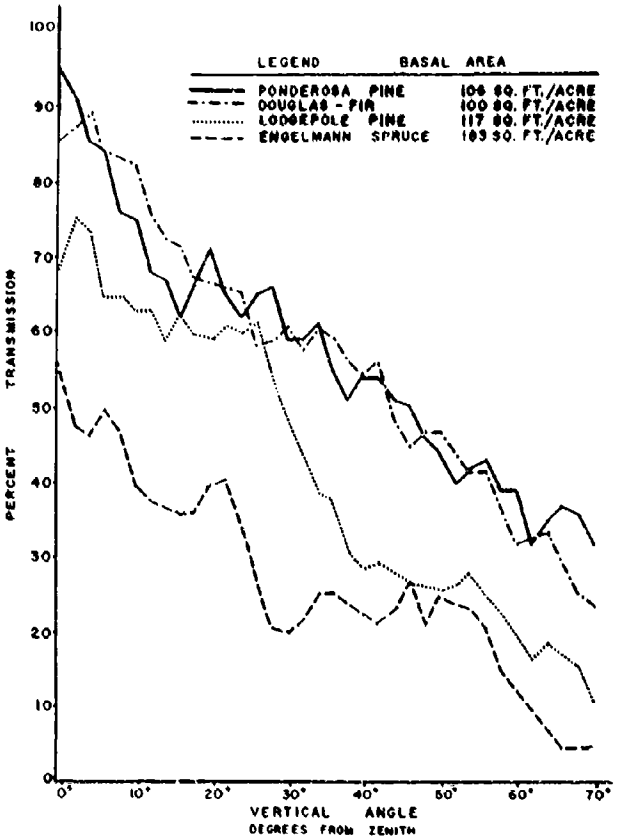

Figure 1. — Percent transmission versus vertical angle for four coniferous species.

because of the high degree of coordination required between the scanner operator and the pilot. A technique of flying compass bearings from visible reference points approximately 4 miles from the test area was more satisfactory. Flight passes were flown from two checkpoints such as towns, ranger stations, or other landmarks that were identifiable during night operations.

Because these test flights were exploratory, many variables were introduced that were eliminated in later test design. Detectors were changed during flights, altitude was not held constant, and equipment settings were not optimized. These factors made it possible to draw only general conclusions from the data.

Imagery obtained from flight tests was examined on a microfilm reader, and the flight passes containing usable data were analyzed. Identification of individual targets depended

upon recognizing landmarks or observation of enough targets to recognize the 4 by 5 pattern. The interpreter was required to use considerable judgment in extracting data from the film strips. Target signatures on the images were often questionable because of improper film exposure. The film density was too dark if video levels were set too high.

The percent of targets detected was used as the dependent variable in evaluating the separate effects of stand density, forest type, altitude, vertical angle, and horizontal ground distance.

A summary of detection results of the three timber types is shown in figure 2. Targets in ponderosa pine and Douglas-fir were detected easily at vertical angles less than 10°, but in the Engelmann spruce detection was only 50 percent. Detection in spruce is very low for angles greater than 30°; however, 40- to 50-percent detection was observed for the other two types. During the four flights represented by these data, no targets were detected beyond 40° except in the Douglas-fir stand, where 33 percent were detected between 40° and 50°. None of the detection data in this report are corrected for the inherent dependence of slant range and Lambertian effects on aspect angle (see scanning geometry, Appendix IV).

A single mission, flown in cooperation with the Infrared Physics Laboratory, Institute of Science and Technology, University of Michigan, indicated their 2-milliradian scanning system would consistently achieve better results; this was especially true in the denser portion of the stand (fig. 3).

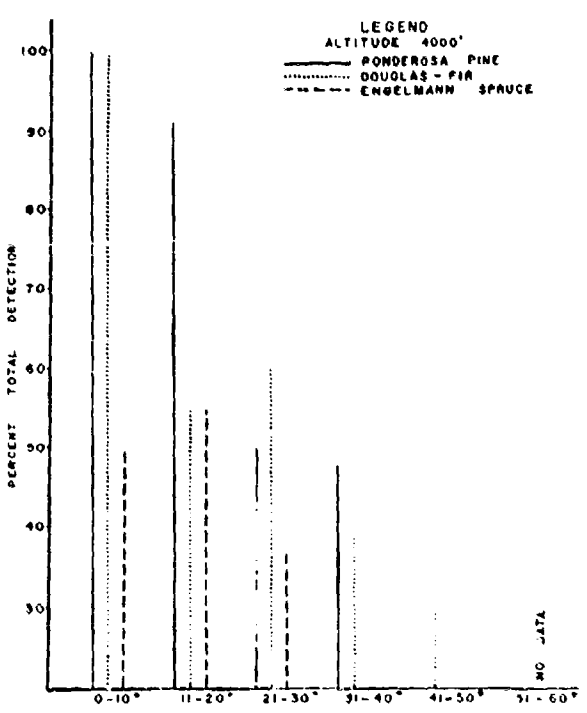

Figure 2. — Percent total detection versus vertical angle for three timber stands.

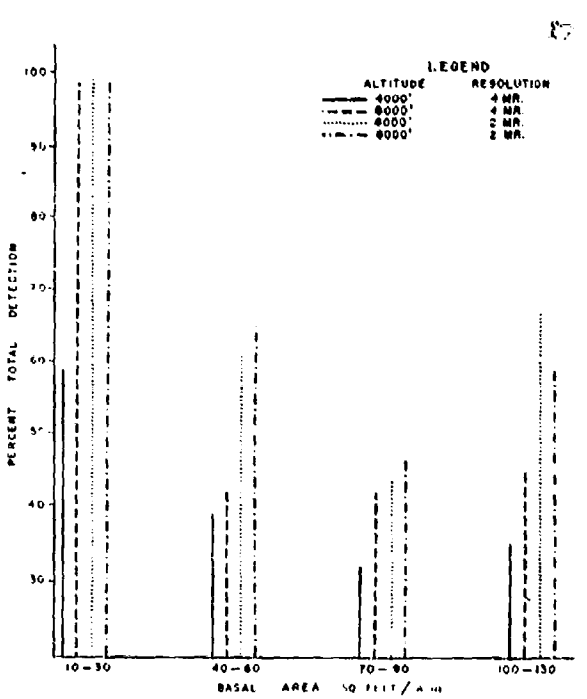

Figure 3. — Percent total detection versus basal area classed for three altitudes and two system resolutions.

The effects of increased stand density and vertical angle were examined by using the data from all altitudes and timber types. This lumping of data was necessary because of the small sample size. These data showed: (1) The extremely low probability for detecting targets in the densest plots for vertical angles greater than 30°; and (2) the difficulty encountered at angles greater than 50° in all but the least sparse portions of the stand.

SUMMARY, PHASE I

The first season's work produced very few definitive results. The problem was attacked with the information and instrumentation at hand, and both proved inadequate.

Deficiencies included: (1) The shortage of pertinent timber canopy ground truth, (2) crude navigational procedures, (3) inadequate data readout, and (4) very poor infrared system sensitivity and resolution.

Positive results were: (1) The project personnel were initiated into airborne infrared experimentation, and (2) personnel obtained a better knowledge of specific program requirements. Using this background knowledge, reasonable program goals were formulated and the necessary modifications of instrumentation were determined.

PHASE II TEST PROGRAM

INTRODUCTION

Objectives of Phase II were to implement the modifications suggested by the Phase I results, and to make quantitative measurements of fire detection probability in the representative timber types. Test plans were made incorporating the necessary revisions. Arbitrary goals of 90-percent detection probability and 10-mile-wide coverage were established as realistic objectives for fire patrol.

DEVELOPMENT OF EQUIPMENT

Experience gained during the 1962 test program demonstrated the need for a higher resolution scanner. Replacement of the standard 35 mm. recording camera with a Polaroid camera facilitated control of image quality. A wider scan angle was needed to eliminate the need for offsetting the scanner. The original scanner was modified to provide 120° scan angle by machining a slot on each side of the scanner housing and modifying the scan-sweep trigger circuitry.

Adding a housing extension that holds a 10-inch focal length objective mirror (fig. 4*A*) increased the focal length of the optical system. A higher resolution tube replaced the C.R.T. printer tube. The video amplifiers were modified to provide the necessary bandpass. A modified Beattie Coleman oscillorecord camera, incorporating a Polaroid back (fig. 4*B*) replaced the camera. The Polaroid film pack was mechanically driven perpendicular to the camera axis to provide the vertical sweep. This mechanical sweep drive simulated the conventional 35 mm. strip film drive. Addition of a 1/4- by 1/4-millimeter indium antimonide detector produced a calculated system resolution of 1 milliradian.

The mount built in the nose escape hatch of the AT-11 aircraft provided for two modes of operation. The normal mode of operation placed the scanner in a fixed vertical position to attain a full 120° scan. The scanner also could be manually rotated around the lateral axis to direct the scan plane forward of the vertical to a maximum "tilt" angle of 60°. The latter provided variation of the aspect angle while repeatedly flying the same flight path directly over the target area. This eliminated the need for offsetting the aircraft flight paths — an extremely difficult task to accomplish accurately.

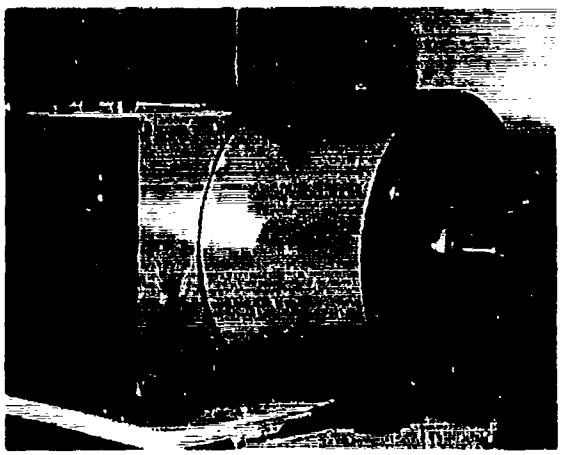

A

B

Figure 4. — Equipment modification: *A*, Infrared receiver modified to a 10-inch focal length system; *B*, Polaroid image recording camera.

TEST PROCEDURE

The Phase I timbered test areas were selected for diversity of stand density and stand form. The tests produced useful fire detection information, but the limited number of samples precluded good quantitative results.

During Phase I the ability to detect the 1-square-foot targets proved very limited. A target array designed with five 1-square-foot charcoal buckets on the circumference of a circle was judged to reasonably approximate an incipient spot fire. The radius of this circle necessary to make the fire detectable then becomes one of the observables of the program.

The Phase II test stands were selected to eliminate as much variation as possible. The test program proposed flight experiments over light, medium, and heavy density stands within each of the four timber types; however, time restricted the actual tests to one stand within each type.

The number of randomly located targets required to determine detection probability within ±10 percent was estimated to be unreasonably large.[5] The number of targets had to be reduced to a practical number that could be handled in the field. Instead of locating the targets at random, we selected dense locations. Biasing of the target locations by selecting the worst cases provided a basis for establishing a lower limit for detection probability, and thereby eliminated some questions of reliability inherent in a small sample size.

The establishment of a lower limit for detection probability was judged to be a realistic goal for Phase II because of the time and effort required for system modification.

For describing forest stands in this report, it is useful to review forest-type terminology used by foresters. The Society of American Foresters[6] defines forest type as:

> A descriptive term used to group stands of similar character as regards composition and development due to given physical and biological factors, by which they may be differentiated from other groups of stands. The term suggests repetition of the same character under similar conditions . . .

During the test program of 1963, the following types as described in "Forest Cover Types of North America,"[7] were sampled to represent typical western forest types: Type #237 Interior Ponderosa Pine, Type #218

[5] *A discussion of sample size and detection probability is included in the Phase III section.*

[6] *Society of American Foresters. Forestry handbook, p. 6. 24. New York: Ronald Press. 1955.*

[7] *Committee on Forest Types. Forest cover types of North America (exclusive of Mexico). Pp. 42, 46, 48, and 57. Washington: Soc. Amer. Forest. 1962.*

Lodgepole Pine, Type #212 Larch—Douglas-fir, and Type #206 Engelmann Spruce—Alpine Fir (*Abies lasiocarpa* (Hook.) Nutt.).

Species in the types named usually form 50 percent or more of the composition. Predominants are judged on the basis of number of stems in the dominant and codominant classes combined.[8]

During the field season of 1963, four new test areas were chosen to determine the effect of timber cover on probability of detection. Relatively pure stands of ponderosa pine, lodgepole pine, larch—Douglas-fir, and Engelmann spruce—alpine fir were selected which met the following criteria:

1. Timber type must be typical of the descriptions used by the Society of American Foresters.[9]

2. Area must be about 40 acres or larger.

3. Flight path (in either a north-south or east-west direction) must provide for safe aircraft navigation.

4. Vehicular access must be available at each end of the area for placement of aircraft navigational devices.

5. Slopes in the area should not exceed 20 percent.

A test area 1,500 feet long by 1,000 feet wide was delineated on the basis of the above criteria. Within this area the timber was cruised by the variable plot wedge prism (Bitterlich) method. The basal area factor for this cruise was selected to give a 50-percent sample of the standing timber on the site. The cruiser recorded the total height, diameter breast high, percent live crown, and species of each tree selected by this method on each plot within the test area. The number of plots varied because of the characteristics of the stand, but was always sufficient to give an accurate representative sample of the stand according to standard cruise techniques for merchantable timber.

Two sets of cruise data were compiled for these areas — one based on merchantable volume, the description most easily visualized by a field forester; the other including all trees with 4-inch and larger diameters. Merchantable volume probably relates more closely to a stand's detection potential. A complete description of the cruise data is included in Appendix I, and is summarized in table 1.

[8] *Ibid, p. 3.*

[9] *Ibid, pp. 42, 46, 48, and 57.*

Table 1. — Cruise information from Phase II test areas by timber type

Measurement	Test areas			
	Lodgepole pine	Ponderosa pine	Larch - Douglas-fir	Engelmann spruce - alpine fir
Trees per acre	161.2	67.1	120.8	160
Board-foot volume per acre[1]	9,050	5,330	16,923	41,208
Average d.b.h. (inches)	10	14.5	14.9	17.5
Average tree height (feet)	62	58.1	82	86
Average crown thickness (feet)	44	40	47	62
Cumulative stem density (inches per acre)	2,662	6,622	2,224	10,344
Crown cover density[2] (percent)	80	60	80	100

[1] *Scribner log rule was used for all merchantable volumes. Cruise includes all merchantable trees 8 inches d.b.h. and larger (by 2-inch classes).*

[2] *Estimated by aerial photos over test areas.*

A four-man ground crew placed charcoal heat sources within each of the test areas. Five standard target buckets were used in each fire array; total target surface area thus amounted to 5 square feet. The fire array locations, as previously mentioned, were selected within the stand to afford maximum obscuration. The locations were spaced to assure separation of arrays on the imagery and allow target identification. At each location a random compass bearing was determined and the first bucket in the target array pattern placed on this bearing at either 3, 6, 9, 12, or 15 feet from the chosen plot center. The remaining four buckets were then spaced as evenly as tree boles would permit (fig. 5) on the circumference of this circle. Subsequent placing of the buckets on the circumference of larger circles simulated a slow burning fire as it spreads over a larger area.

Aircraft altitude was maintained at 8,000 feet over terrain. Navigation along the flight path was accomplished by visually alining the aircraft with three high-intensity rotating beacons. One beacon was located within the test area and the other two were placed 2 miles from the test area in either direction along the flight path. The equipment operator was aided in starting the Polaroid camera at the proper point by an unobscured signal fire that appeared on the 5-inch monitor as the aircraft approached the area.

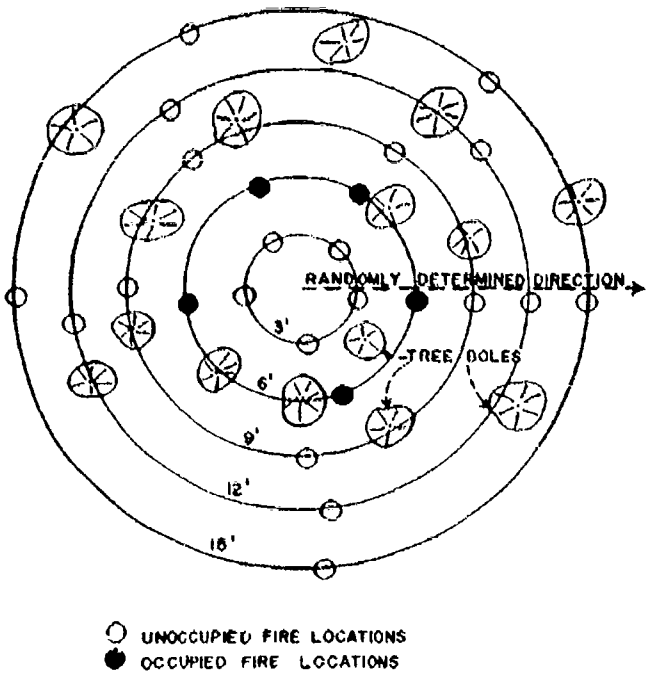

Figure 5. — Fire array target pattern.

Eight fire arrays were used on each test. At the beginning of each test the five buckets were arranged on the circumference of a 3-foot circle. With the scanner oriented straight down, a pair of passes was completed from opposite directions and the imagery examined. If 14 of the possible 16 detections were accomplished, the scanner was tilted forward an additional 10° and the fires viewed from this larger angle on the next two passes. If fewer than 14 fire arrays were detected, the scanner was left in the same position, the fire radius increased by 3 feet and the imagery from the next two passes examined. Fire radius was increased in 3-foot increments and passes were repeated until satisfactory results (14 out of 16 targets) were attained, or until a 15-foot maximum radius circle was reached at each aspect angle. After tests over the eight fire arrays were completed, the fires were moved to eight alternate locations and the test cycle repeated.

DISCUSSION OF RESULTS

If horizontal ground coverage (pathwidths of 10 miles) was to be attained from the normal operational altitude of propeller-driven aircraft, it was essential to accomplish detection at angles approaching 60°. Satisfactory data were limited to vertical angles of 50° in spite of every effort to obtain reliable data on the critical 60° vertical angle. The increment from 50° to 60° was important because of the increased ground coverage per degree at these large oblique angles.

Two samples of imagery of the larch—Douglas-fir test area are shown in figure 6. Figure 6*A* shows the raw data from one of the passes that established the detection probability at 20°. This sample shows successful

A

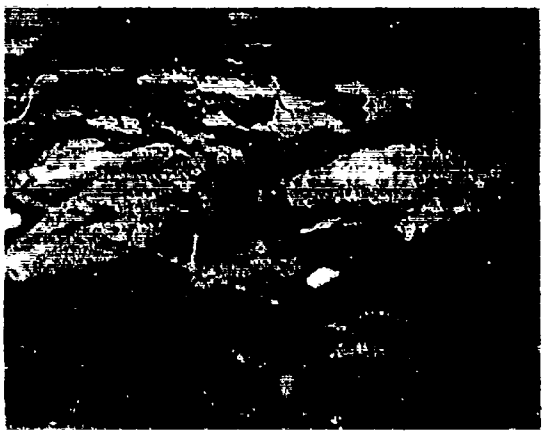

B

Figure 6.—Samples of flight test imagery: *A*, Imagery obtained with scanner tilted at 20°; *B*, imagery with scanner tilted at 50°.

detection of each of the eight fire arrays. Figure 6*B* shows two targets detected at 50°; close examination reveals at least four targets from which radiation penetrated the canopy, yet the system failed to separate them adequately from the background. These four targets were considered submarginal because an image interpreter on a fire patrol mission would have trouble making a positive identification. Marginal targets could be made more prominent by adding a pulse-height discrimination capability to the system.

In an effort to simulate a spreading fire, five 1-square-foot heat sources were placed on a 3-foot-radius circle and subsequently moved by 3-foot-radius increments to a maximum radius of 15 feet.

Data were recorded by fire radius classes, scan angle increments, and flightpass numbers. The raw data were then refined into composite values for each fire radius class within each of the 10° scan angle increments. These data are shown graphically (figs. 7 through 10). This analysis shows an increase in detection probability corresponding to an increase in fire radius. The maximum detection probability occurs in the range between 9- and 12-foot radius fire arrays.

Proper interpretation of these results, as they relate to a spreading fire with hot spots remaining inside the perimeter, excited considerable discussion. An extrapolated percent detection was calculated in the following manner.

For each timber type and aspect angle, the imagery was examined by consecutive 3-foot-radial increments. An individual target array detected at a given fire radius was assumed to be detectable at all larger radii. Positive detection results were accumulated by 3-foot-radial increments at each of the eight target locations in the test area. The final radius at which 90+ percent detection for the test area occurred was recorded for each aspect angle and timber type. Table 2 is a synopsis of the accumulative detection results.

It is important to remember that the 3-foot fire size represents 5 square feet of fire; the 6-foot fire size, 10 square feet of fire; etc. Figures 11 through 14 give the accumulative detection probabilities versus aspect angle for the several test areas. The ratio of detected targets to a total number of targets in the sample is included on each graph.

The detection probability thus measured is conservative. The fire plots were selected in the densest portions of the test stands. This analysis does not account for any energy radiated in less than threshold amounts. The results of this accumulative detection analysis establish lower bound detection probabilities for fires in timber stands similar in density and composition to the test stands.

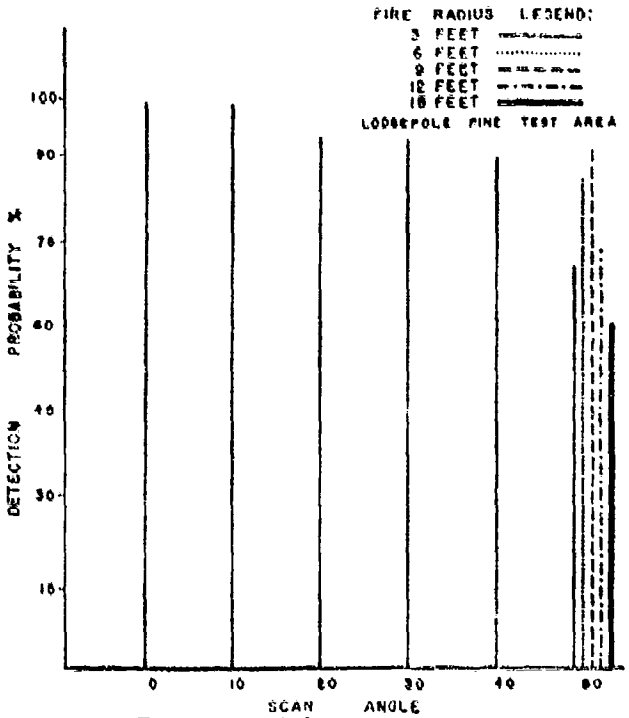

Figure 7. — Detection probability as a function of vertical angle and fire radius for lodgepole pine test area.

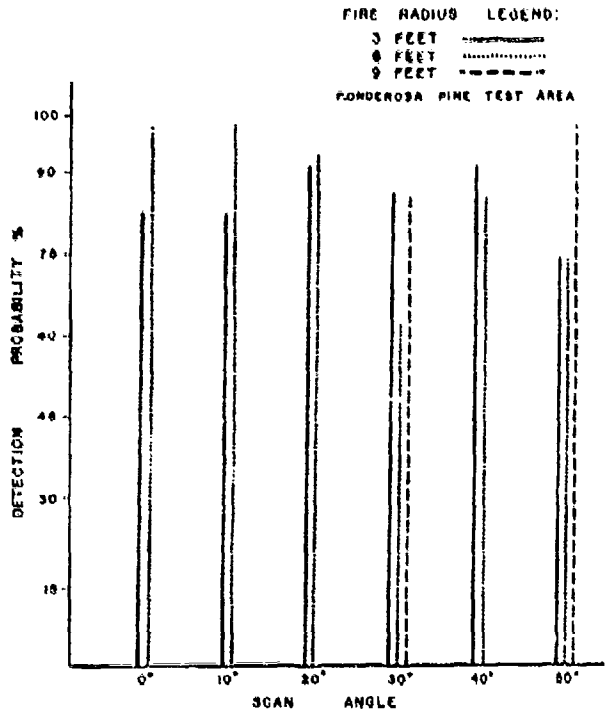

Figure 8. — Detection probability as a function of vertical angle and fire radius for ponderosa pine test area.

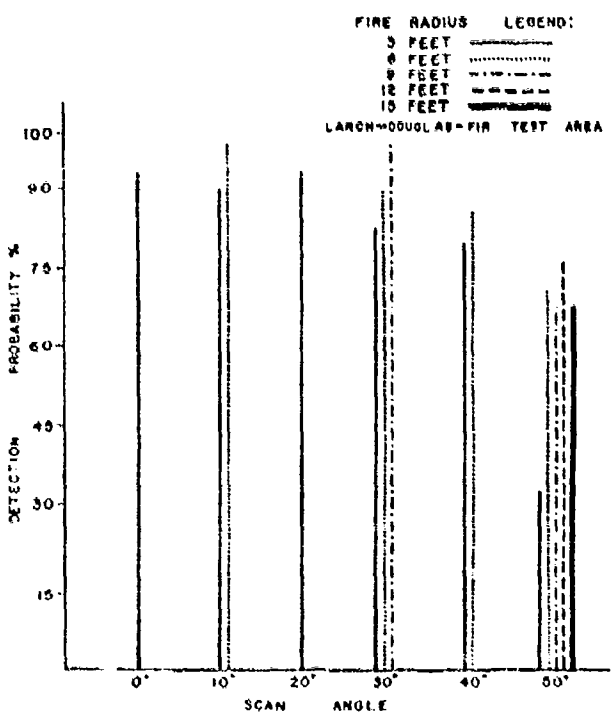

Figure 9. — Detection probability as a function of vertical angle and fire radius for larch—Douglas-fir test area.

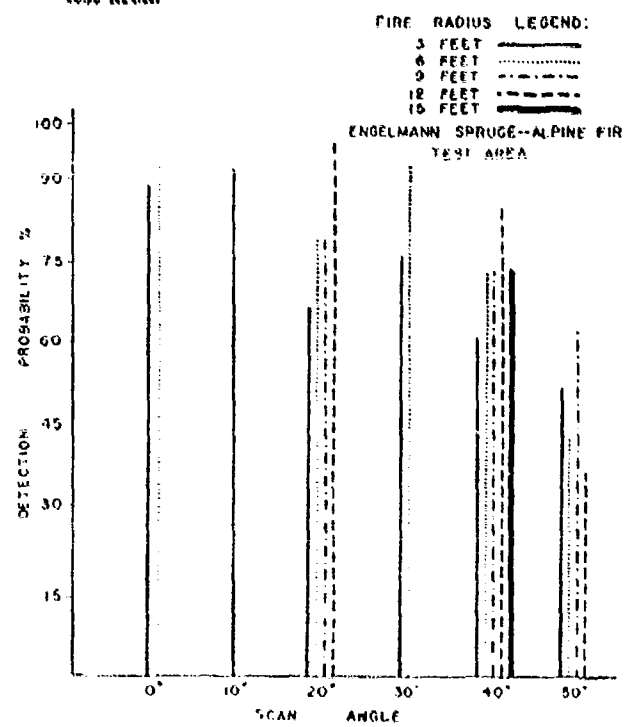

Figure 10. — Detection probability as a function of vertical angle and fire radius for Engelmann spruce — alpine fir test area.

Table 2. — **Accumulative detection results for multiple target configurations**

Species	Detection results		
	Fire size	Scan angle	Detection probability
	Feet	Degrees	Percent
Lodgepole pine	3	0-40	90+
Lodgepole pine	6	40-50	90+
Ponderosa pine	3	0-40	90+
Ponderosa pine	6	40-50	90+
Larch - Douglas-fir	3	0-20	90+
Larch - Douglas-fir	6	20-50	90+
Engelmann spruce - alpine fir	3	0-10	90+
Engelmann spruce - alpine fir	6	20-30	90+
Engelmann spruce - alpine fir	9	40-50	90+
Engelmann spruce - alpine fir	12	50	80—

Preliminary results of the studies of target fire detection in the vario timber types indicated detection probabilities were lower in the denser timber types and higher in the lighter types. However, within each stand there existed several qualitative ambiguities between percent detection and timber canopy characteristics that were visually estimated. To resolve these difficulties, the timber canopy of one test area as studied in more detail.

At the larch—Douglas-fir test area, the canopies in the immediate vicinity of each of the 16 target arrays were examined. Measurements included d.b.h., tree height, percent live crown, and profile of individual tree boles.

No correlation existed between the canopy measurements and the flight data.

The major difficulty in determining significant factors of timber canopy obscuration was the inability of the ground crew to determine the precise optical path through the canopy at the moment the test plot was in the field of view of the scanner. A more detailed study of canopy obscuration could be made from an elevated, fixed-scanner platform.

Plans were made to fly simulated patrol missions before the start of the fire season. The aircraft was equipped with a dual-omni navigation system. The pilot was to fly compass bearings between checkpoints that were to be calculated by triangulation from two known omni stations. During several simulated missions, this technique proved inadequate for navigation over a contiguous strip-patrol pattern.

Charcoal fires were placed within the patrol area at locations unknown to the aircrew. The aircraft navigated omni fixes and compass bearings and attempted to follow designated north-south paths. The scanner operator monitored the infrared image on the face of a 5-inch scope for potential fire targets. The potential fire locations were not recorded on film because the Polaroid camera, being a single-frame camera, could not obtain continuous real-time imagery. When a potential target was observed on the monitor, the pilot was instructed to start a standard figure-eight flight pattern. This maneuver placed the aircraft over the potential fire twice more with the final leg being a continuation of the original course. By keeping track of elapsed time, the operator was to record the imagery over the potential spot fire. This procedure was not satisfactory because the timing and coordination necessary

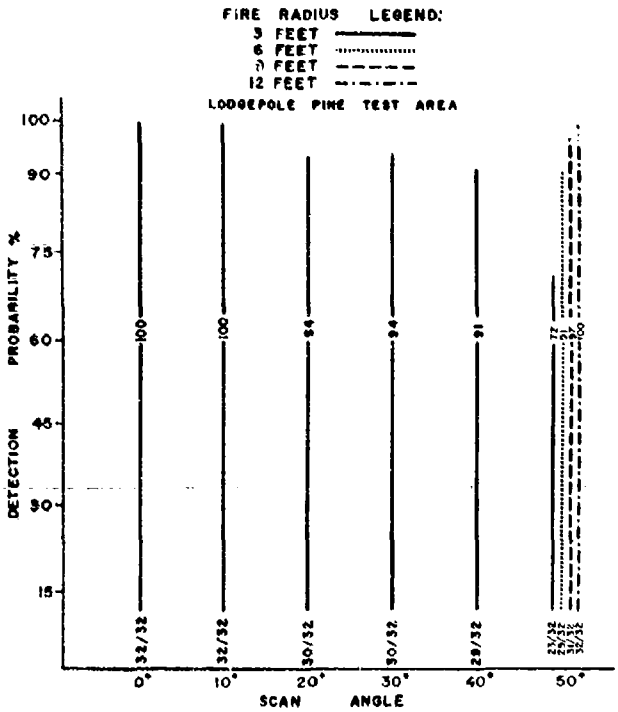

Figure 11. — Accumulative detection probability versus vertical angle and fire size for lodgepole pine test area.

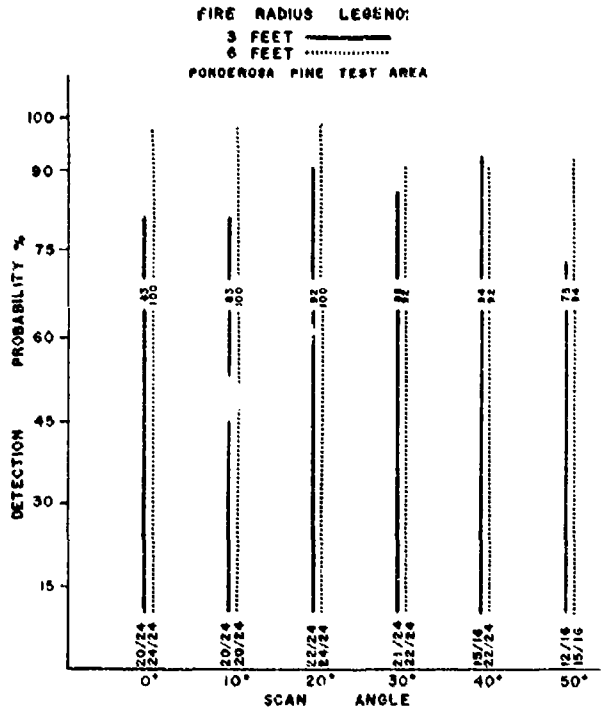

Figure 12. — Accumulative detection probability versus vertical angle and fire size for ponderosa pine test area.

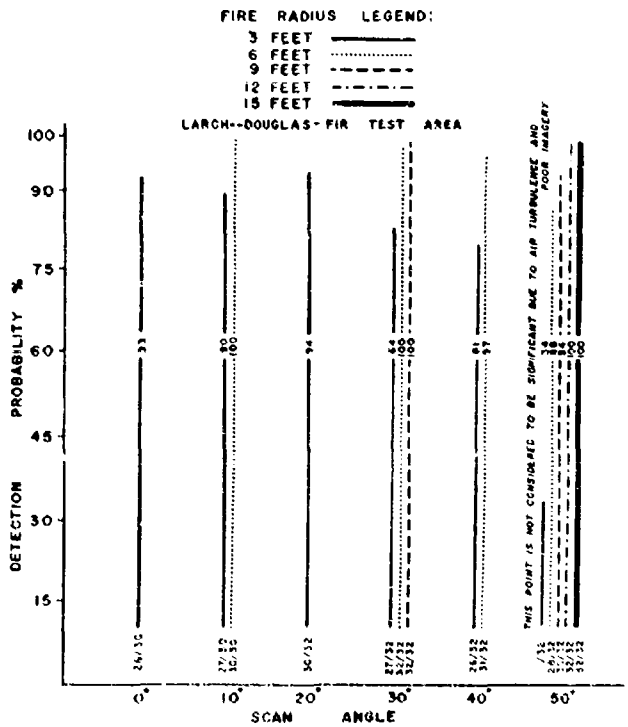

Figure 13. — Accumulative detection probability versus vertical angle and fire size for larch—Douglas-fir test area.

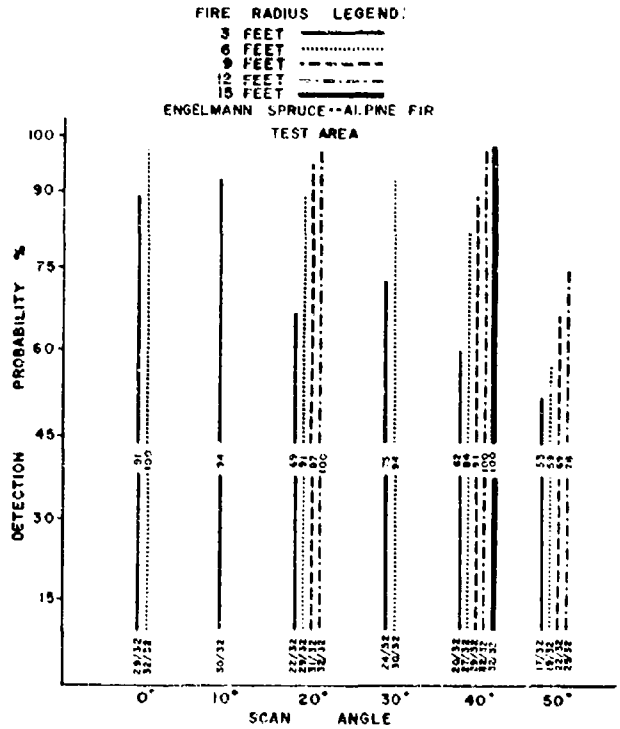

Figure 14. — Accumulative detection probability versus vertical angle and fire size for Engelmann spruce — alpine fir test area.

to precisely locate the target area during the maneuver could not be achieved.

One mission detected one out of five charcoal fires (each was a five-bucket array) placed in the 900-square-mile patrol area. The ground crew observed that the navigation techniques used did not place the aircraft in position to detect the remaining four. Four other hot spots were detected on the mission, however; these targets coincided with known campground locations. The one test fire detected was accurately located through use of infrared imagery and existing aerial photographs. The fire detection patrol flights during Phase II demonstrated that the relatively simple navigation techniques used will not satisfy patrol requirements.

The Beechcraft AT-11 aircraft was unable to operate at 15,000 feet above terrain, the altitude needed to attain 10-mile-wide coverage utilizing a 120° scan. Limitations on aircraft fuel and oxygen supply made attempts to perform extended high altitude tests impractical. The aircraft could not attain altitudes necessary to investigate the detection limits for unobscured 5-square-foot sources. The unheated, unpressurized, and cramped instrumentation space seriously degraded the performance of the equipment operators.

SUMMARY, PHASE II

At the end of Phase II many factors were evident that affected the realization of the project goals. Their scope is best presented in the following outline:

1. Accomplishments

a. Equipment performance and data acquisition techniques provided reproducible detection measurements.

b. Information about detection probability was obtained for the four representative coniferous timber types.

c. A qualitative list of requirements for an operational system was being acquired.

2. Problems yet unsolved

a. Instrumentation and navigation problems limited the detection data to aspect angles of less than 50°.

b. The large number of submarginal target observations indicated inadequate system sensitivity.

c. The high speed nature of flight tests does not facilitate precise observation of timber obscuration factors.

d. Aircraft navigation and altitude capabilities of the present aircraft are inadequate.

3. Proposed equipment modifications

a. An aircraft capable of flying at higher altitude and providing at least a minimum of operator comfort must be acquired.

b. The aircraft must have a better navigation capability.

c. The scanner system modifications should include:

(1) an increased electronic bandpass,

(2) the addition of a pulse-height discrimination circuit, and

(3) the addition of a rapid process, continuous strip photographic readout.

4. Proposed program modifications

a. The technical competence of the project should be broadened by acquiring additional professional personnel, including U.S. Forest Service pilots and technical personnel.

b. Experimental reorganization should include:

(1) the addition of a mountaintop-fixed platform study of canopy obscuration parameters and

(2) the division of the flight program into two separate studies:

(a) Fire detection studies in the various timber types and

(b) Wildfire patrol and navigation problems.

PHASE III TEST PROGRAM

OBJECTIVES

The goals of the 1964 season, delineated in a test plan, are summarized as follows:

1. The infrared system modifications were to be checked out. Correlation was to be established with previous test results by reruns on the lodgepole pine test area. Data gathering and flight test operational procedures were designed similar to those of Phase II.

2. When equipment performance proved satisfactory, flight tests were to be run on white pine (*Pinus monticola* Dougl.) and coastal Douglas-fir. Also, flight measurements were to be extended to 15,000 feet over terrain and 60° aspect angles in representative timber types. This would complete the preliminary survey of fire detection probabilities for northwestern coniferous timber types.

3. During the lightning fire season (July 15 to September 1) the problems of fire patrol were to be investigated. The immediate goals included familiarization with the navigation system and comparison of effectiveness of infrared surveillance with present Forest Servive methods. Observations were to include the feasibility of early detection of incipient fires and immediate dispatching of fire suppression forces.

4. After the lightning season, the scanner was to be removed from the aircraft and mounted at the previously selected mountaintop-fixed platform test site. The mountaintop program included: (1) Extension of the larch—Douglas-fir detection probability curve to beyond 60° and (2) the detailed investigation of forest canopy obscuration factors.

FIRE DETECTION TESTS

A Convair T-29 aircraft, equipped with a Doppler radar navigation system, was acquired on loan from the U.S. Air Force. The infrared instrumentation was modified as proposed at the conclusion of the 1963 program and installed in the aircraft.

The first instrumentation checkout flight was not made until June 22, primarily because the Convair T-29 aircraft arrived late. On June 24, the first extended night checkout flight proved very encouraging. The aircraft and radar navigation system performed beautifully. The electronic instrumentation seemed adequate at that time. Intermittent use of the pulse-height discrimination circuit indicated satisfactory performance.

On June 25, the first attempt was made at reproducing 1963 data for the lodgepole pine test area. The scanning system included a new rapid process, continuous strip photographic readout (moving window display), and a modified video electronic system. Preliminary system sensitivity measurements were marginal. During the first week in July, a new high resolution cathode ray tube was installed in the moving window display. This modification worked very well and the photoprocessor readout continued to perform impressively for the rest of the season.

In the middle of July the aircraft's electric, hydraulic, and navigation systems became unreliable. During the next two months the aircraft went through five extensive maintenance periods.

The flight test program continued through July and into August. Tests were made in the lodgepole pine test area and the white pine test area at Priest River, Idaho. A single fire patrol mission was flown on August 21. The infrared receiver and video electronics continued to demonstrate intermittent reliability because of excessive modification.

During the third week of August it was apparent that continued efforts to increase the sensitivity of the present electronic and receiver system would not succeed. Flight operations were terminated and the instrumentation removed from the aircraft.

Bench tests of the infrared receiver indicated it would still operate satisfactorily in a stable ground environment. It produced satisfactory results during the mountaintop test series.

FIRE PATROL

Equipment and Test Procedure

The Doppler navigation system, which reads out directly in latitude and longitude, provided a suitable navigation capability. Specifications for the accuracy of Doppler systems are commonly within 2 percent of track. If this accuracy could be attained, the Doppler system would keep the aircraft within 2 miles of the proposed flight path on a 100-mile patrol run. This accuracy is near limits which could be tolerated on patrol missions.

A 1:60,000 aerial photomosaic was made of the proposed patrol area and used as a navigational aid. The photomosaic was cut into strips that included the area to be covered on each patrol run. Latitude and longitude lines were marked on the photostrips to describe locations.

The moving window display provided rapidly available strips of infrared imagery that could be compared to the aerial photomosaic to determine aircraft location.

During the detection missions it became evident that cumulative errors in the Doppler system would exceed the accuracy requirements for patrol work. Infrared-aerial photo-interpretation could not provide the precise information in reasonable time for patrol navigation. A combination of the two systems offered a better chance for success. Plans were made to navigate with the Doppler system, and to use the comparison of the aerial photo-infrared imagery to determine periodically true aircraft location. True location provides a basis for correcting accumulated errors in the Doppler system. If navigational procedures worked satisfactorily, patrol missions would be flown after periods of lightning activity.

Patrol Area

A 6,000-square-mile patrol area southwest of Missoula was selected because it was sparsely populated and had a history of frequent lightning occurrence. A sparsely populated area is less likely to give false alarms attributable to campers, vehicle exhaust, and similar disturbances. The 60-mile-wide patrol area was bordered on the east by a 100-mile line extending from Alberton, Mont., south to the Salmon River.

The area was divided into seven 8-mile-wide patrol strips. This width was chosen to give ample overlap on adjacent passes, and to provide simplicity for navigation because adjacent flight lines would be separated by 10-minute increments of longitude.

At least three prominent topographic features, such as road intersections or lakes, were selected on each proposed flight path to serve as checkpoints for purposes of establishing true location during the flight.

Patrol Flight

A single patrol was flown on August 21. The aircraft's operational ceiling of 18,000 feet m.s.l. limited the flight altitude to 12,500 feet over average terrain. At this altitude the 120° scan angle gave 4-mile coverage to either side of the flight path.

During the first pass, on a southerly heading along strip 1, we relied on the Doppler system entirely. The aircraft began the pass on course and drifted consistently to the west. This drift was detected by comparing the infrared image to the aerial photomosaic. When the pass was completed, the Doppler navigation was corrected by addition of 4 minutes longitude. The pilot was able to correct his heading on the second pass and the drift was eliminated.

The Doppler and scanning equipment were both functioning poorly during the flight; however, it was still possible to navigate the desired course. Patrol flights were terminated at this point because of equipment troubles.

MOUNTAINTOP TESTS

General Discussion

A fixed-mountaintop scanner site was established to examine in detail those factors which obscure targets and extend detection data beyond the critical 60° (fig. 15).

Two advantages of a fixed site are: (1) Operation is more economical and (2) test measurements can be observed for a much longer time than is possible from a fast moving aircraft.

The only location with suitable elevation (aspect angle) and timber stand within reasonable distance of Missoula is in the Bear Creek Drainage west of Victor, Mont. (fig. 16). This precipitous area provides: (1) Vertical aspect angles between 45° and 70°, (2) slant ranges of 3,400 to 7,400 feet, and (3) a well-stocked mature larch—Douglas-fir stand associated with grand fir, Engelmann spruce, and alpine fir.

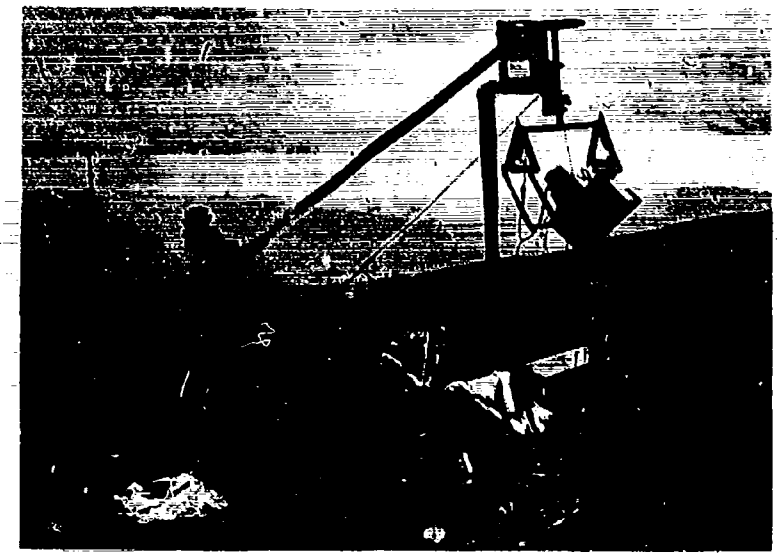

Figure 15. — Mountaintop scanner installation.

Figure 16. — Test area from scanner location.

Preparation of Program

The mountaintop test was designed to supplement and extend the results of the flight program. Lack of previous experience made the first effort largely a trial run, and most procedural details were worked out on the spot. The initial objectives of the program were:

1. The detection probability curves were to be extended to larger aspect angles. Flight program data had been limited to angles less than 50°.

2. The spatial distribution of sizes and types of canopy obscurations was to be determined over an extended area.

3. The effects of background temperature, target emissive area, and scanner field of view on the target-to-background signal (S_T/S_B) ratio were to be determined.

4. Identifiable foliage and timber patterns were to be related to detection probability and signal strengths.

5. Correlation was to be determined between target signal strengths and detection probability.

Test plots at angles between 45° and 60° at 2° intervals were planned. Plot locations were chosen to provide a homogeneous timber canopy. Each plot was 100 feet long and oriented at right angles to the scanner azimuth (fig. 17). The ground was cleared of obstructions for access and preliminary timber cruise data were taken for each plot. Test plots were initially prepared at 45°, 50°, 52°, 54°, 56°, 58°, and 60°, but because of ambiguities in preliminary data at these plot locations, additional plots were constructed at 51°, 53°, 55°, 56½°, 57°, 60½°, 61°, and 69°.

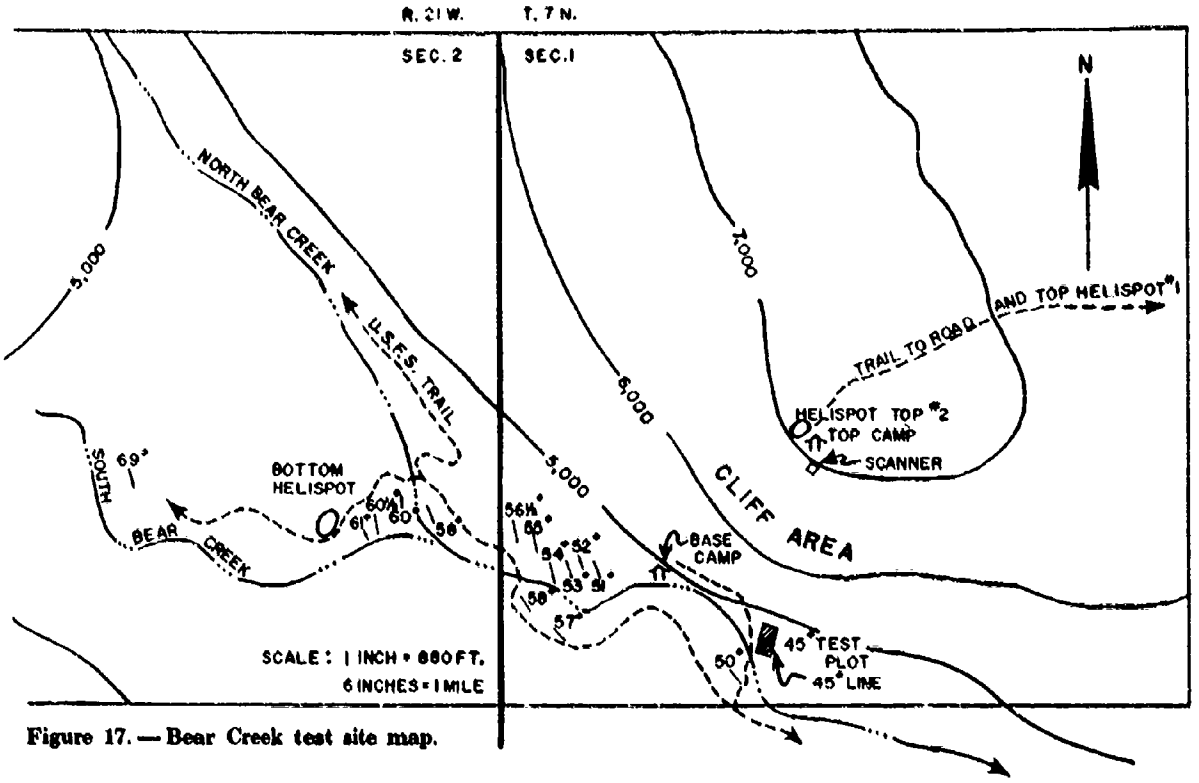

Figure 17. — Bear Creek test site map.

To facilitate detailed canopy measurements, a two-dimensional plot (50 feet by 200 feet) at the 45° aspect angle was prepared.

Instrumentation

Figure 18 is a block diagram of the scanner instrumentation. The video electronics used during the flight program were discarded and simple video amplifiers substituted. This provided an adequate but much less sophisticated video electronic and readout system. The scanner was mounted so that the scanning sweep started 30° above the horizon and swept down through 120° of elevation angle to the vertical. The scanning mirror rotated at approximately 3,600 r.p.m. and gave two scan sweeps per revolution. Precise control of scanner azimuth allowed detailed observation of individual optical paths. Relative radiant intensity was measured in volts at the oscilloscope. Rough system calibration is described below.

To eliminate the effects of reflected solar radiation, radiometric test measurements were made only at night (1930 hours to 2400 hours). A 100-watt incandescent light was located close to the scanner so that the crew on the target area could locate the scanner at night and make subjective estimates of canopy obscuration.

The test targets were 14-inch diameter (1.07 square feet) fire buckets, each filled with approximately 10 pounds of burning charcoal briquettes. The same sources are used in the flight program and have proved to be near black body, Lambertian radiators.

Figures 19 and 20 are representative Polaroid photos of the oscilloscope readout. Table 3 gives measurement data for each illustration. Figures 19*A* and *B* show the change in background signal level over the 5-3/4-hour period just after sunset. Figures 19*C* and *D* are of the same 1/16-square-foot calibration target. In figure 19*C* the labeled points indicate (A) the beginning point of scanner sweep, (B) the horizon, (C) target signal spike, and (D) end of sweep. The space D to A′ is sweep dead time before the beginning of the next sweep at A′. On 19*D* the sweep was expanded and delayed for more precise signal observation.

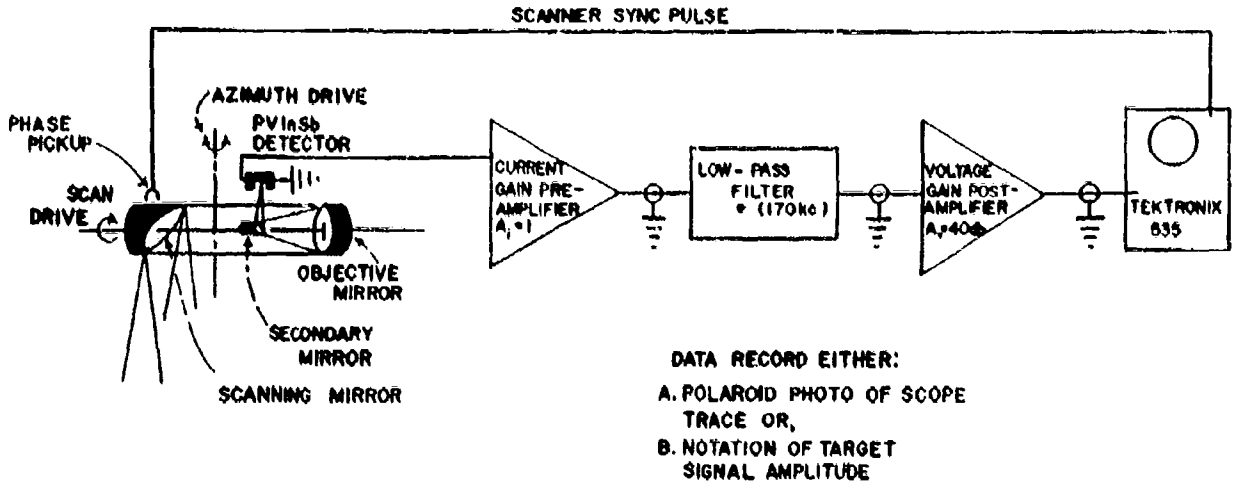

Figure 18. — Block diagram of mountaintop scanner instrumentation.

Figures 20*A* and *B* indicate enhancement of system signal-to-noise (S/N) ratio by use of electronic filtering with 12 db per octave rolloff above 150 kc.

Figures 20*C* and *D* are measurements of scanner resolution; two 12-briquette fires were placed 1.7 milliradians and 2.6 milliradians apart, respectively, along the scanning line.

On-the-spot calibration was provided by signals from line arrays of a small number of individual 1-3/4-inch-square glowing briquettes. Figure 21*A* is a typical calibration curve (in this case from 50° plot); 0.2 volt was the observed signal from one briquette, and 2.5 volts was the signal from 12 briquettes. The system saturated at approximately 3.5 volts (fig. 21*B*, taken at 69° plot), indicating lack of ufficient dynamic range in the voltage gain post amplifier. Compensation is necessary for slant range and Lambertian effects between calibrations at the different test plots.

Rough calculations from inadequate calibration techniques indicate: (1) The total radiant emission from the standard targets is approximately 1.7 watts/cm², or about 35 watts per briquette; (2) the "calibration" on the linear portion of the response curve in the spectral region of measurements gives a system output voltage response to effective target emission of 0.125 volt/(watt/steradian).

Table 3. — Measurement parameters associated with figures 19 and 20

Figure no.	Signal	Sweep scale		Date	Time of day
		Time	Scan angle		
	Volts/div.	Sec./div.	Degree/div.		
19*A*	.2	2 msec.	45.0	10/13	1825
19*B*	.2	1 msec.	22.5	10/14	0012
19*C*	.2	1 msec.	22.5	9/28	1850
19*D*	.2	50 μsec.	1.12	9/28	1853
20*A*	.2	50 μsec.	.45	9/14	2255
20*B*	.2	20 μsec.	.45	9/14	2250
20*C*	1.0	10 μsec.	.22	9/16	—
20*D*	1.0	10 μsec.	.22	9/16	—

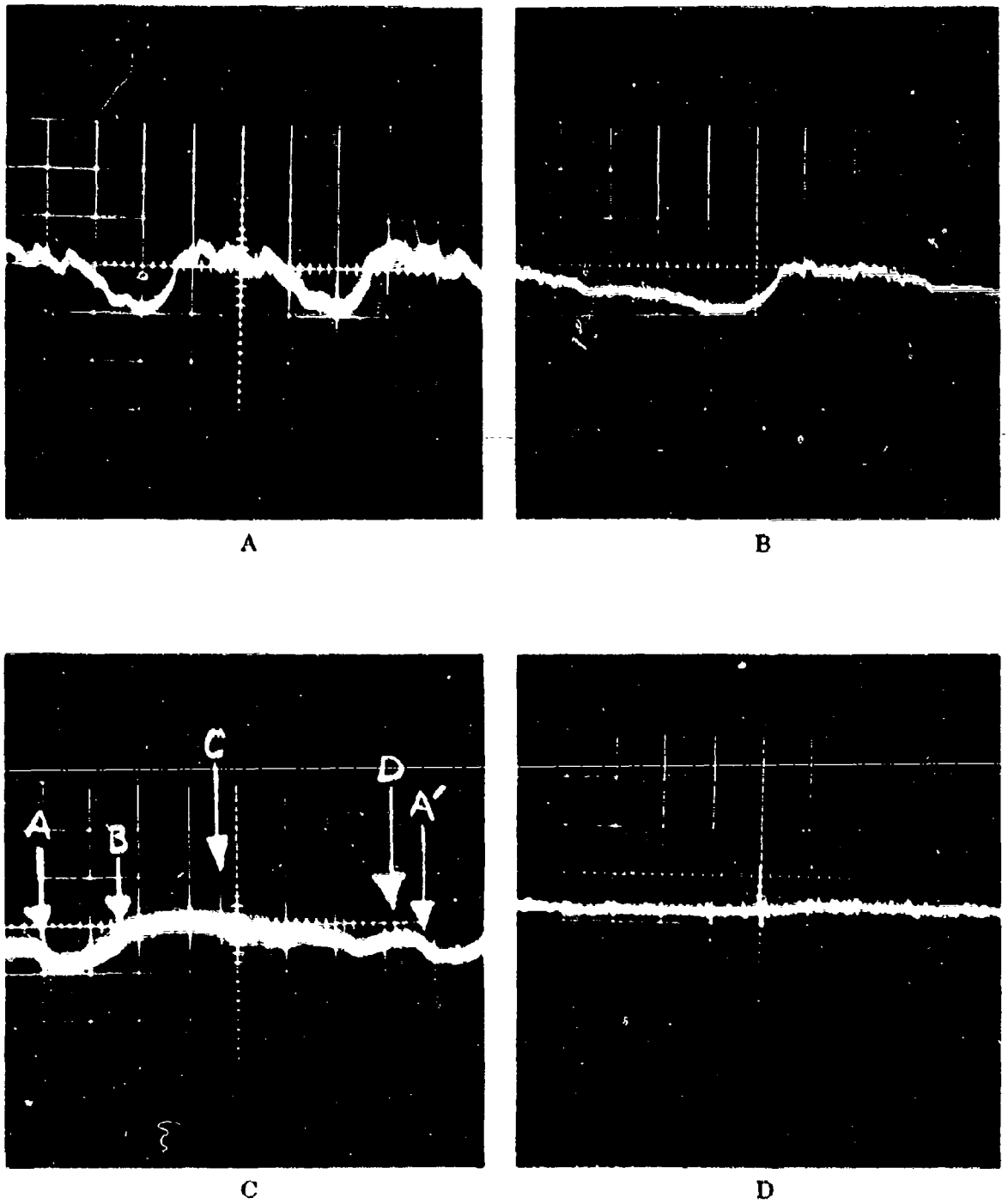

Figure 19. — Polaroid photographs of oscilloscope readout: *A* (1825 hours, 10/13) and *B* (0012 hours, 10/14), change in background signal level over a 5-3/4-hour period; *C* and *D* (1/16-square-foot target), full scan sweep on *C*, sweep expanded and delayed for more precise signal observation on *D*.

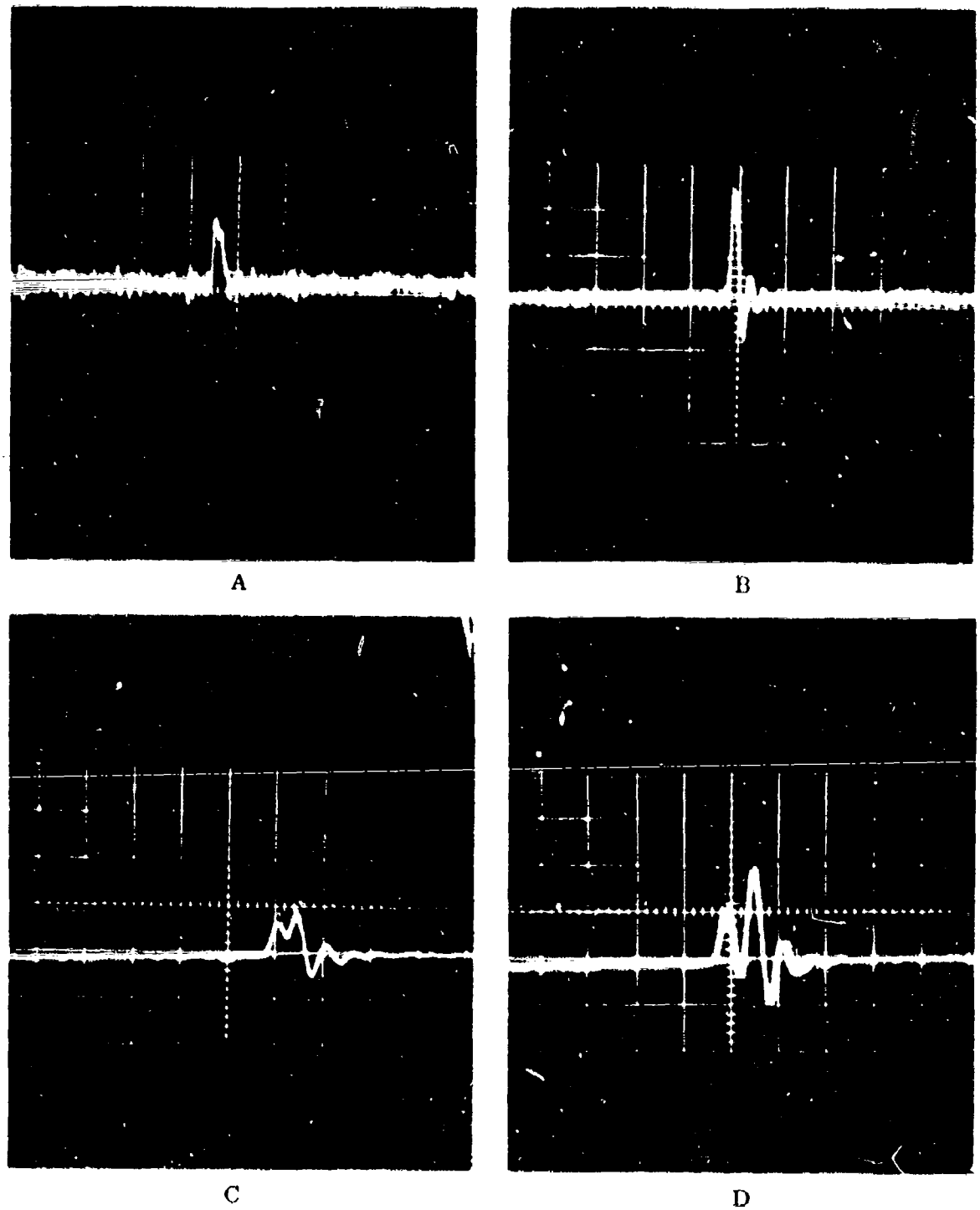

Figure 20.—Polaroid photographs of oscilloscope readout: *A*, target (35, 75) signal and system noise with no electronic filter; *B*, same sweep with 150 kc. low-pass electronic filter; *C*, measurement of scanner resolution, two fires 1.7 milliradians apart; *D*, measurement of scanner resolution, two fires 2.6 milliradians apart.

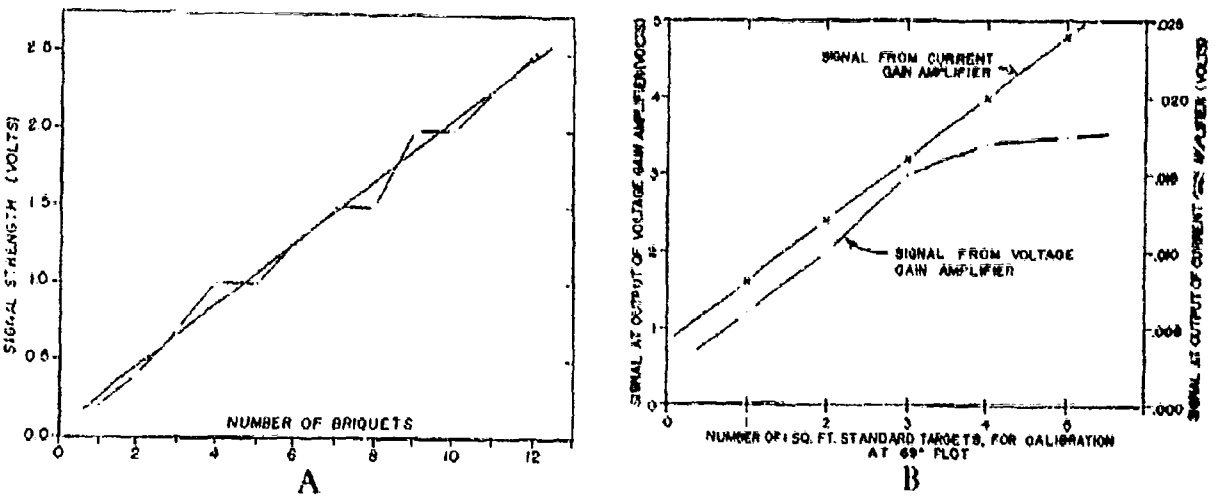

Figure 21. — *A*, Instrument calibration curve; *B*, calibration curve showing nonlinear response of the voltage gain amplifier.

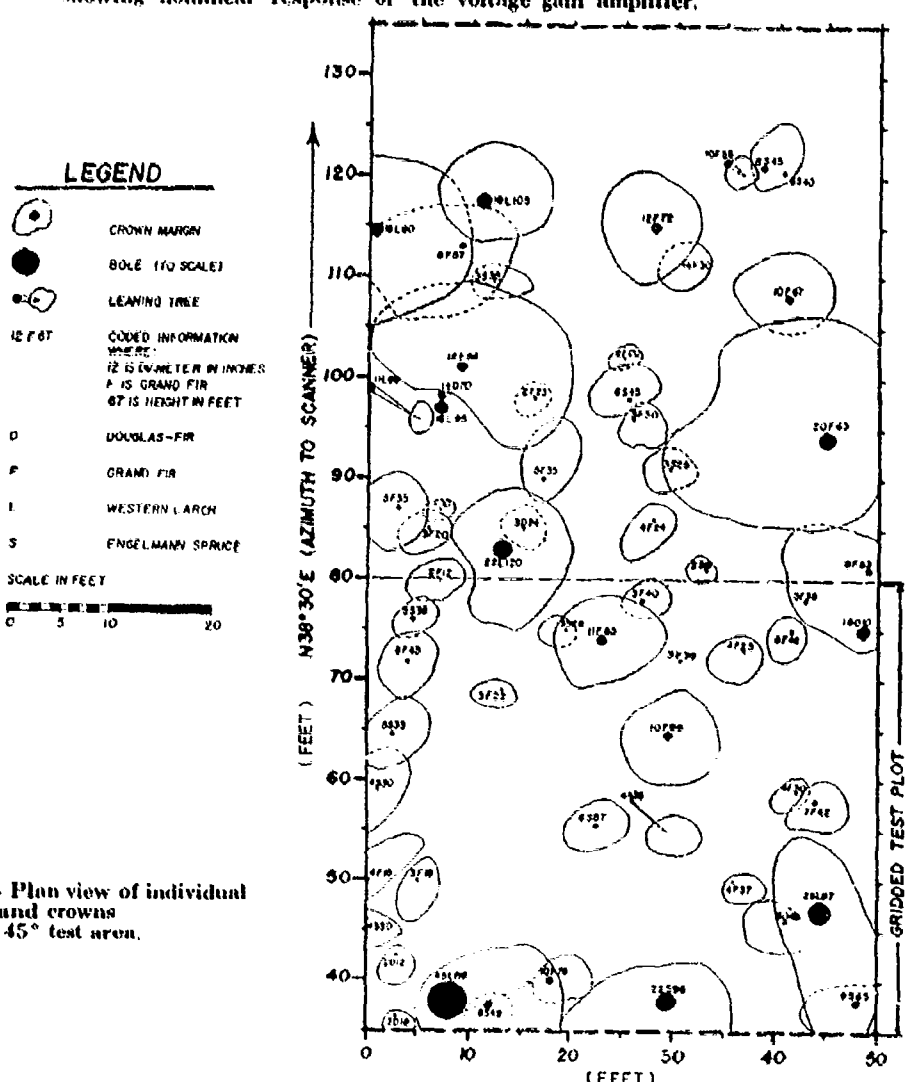

Figure 22. — Plan view of individual tree boles and crowns within the 45° test area.

Discussion of Tests at 45° Plot

This plot was prepared to observe the exact nature of the timber canopy obscuration. A gridded plot was laid out (45 feet by 50 feet) to encompass "several representative tree crowns." A plan view was made of all tree crowns and boles which would obscure any portion of the test plot (fig. 22). For this purpose it was necessary to include trees up to 65 feet in front of the gridded area.

The 45° plot grid locations are referred to by the abscissa and ordinate, respectively, of figure 22, and have the dimensions of feet from the extreme southwest corner of the test area.

Radiation measurements (i.e., scanner signal voltage) were made from a 1.07-square-foot target placed successively at each 1-square-foot grid increment throughout the 45- by 50-foot plot. Figure 23 shows a signal voltage profile of the 45° area. Signals were recorded by 0.1-volt increments. The only system calibration available is that which was extrapolated to 45° from the 50° plot. For the qualitative nature of this report the 50° calibration curves are adequate for the 45° data. For precise extrapolation to 45°, multiply the abscissa of the 50° calibration curves by 1.33 (fig. 21*A*).

In addition, a limited number of larger fire arrays was investigated to determine the

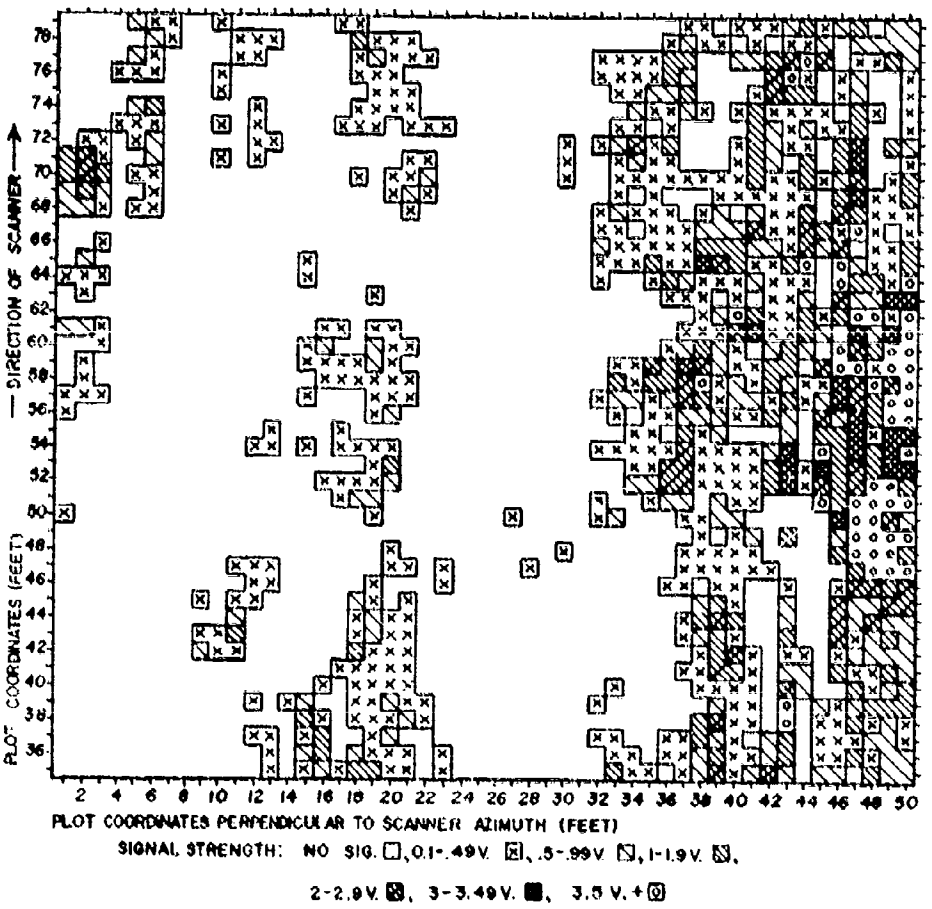

Figure 23. — Signal voltage profile of 45° test area, from 1-square-foot charcoal sources.

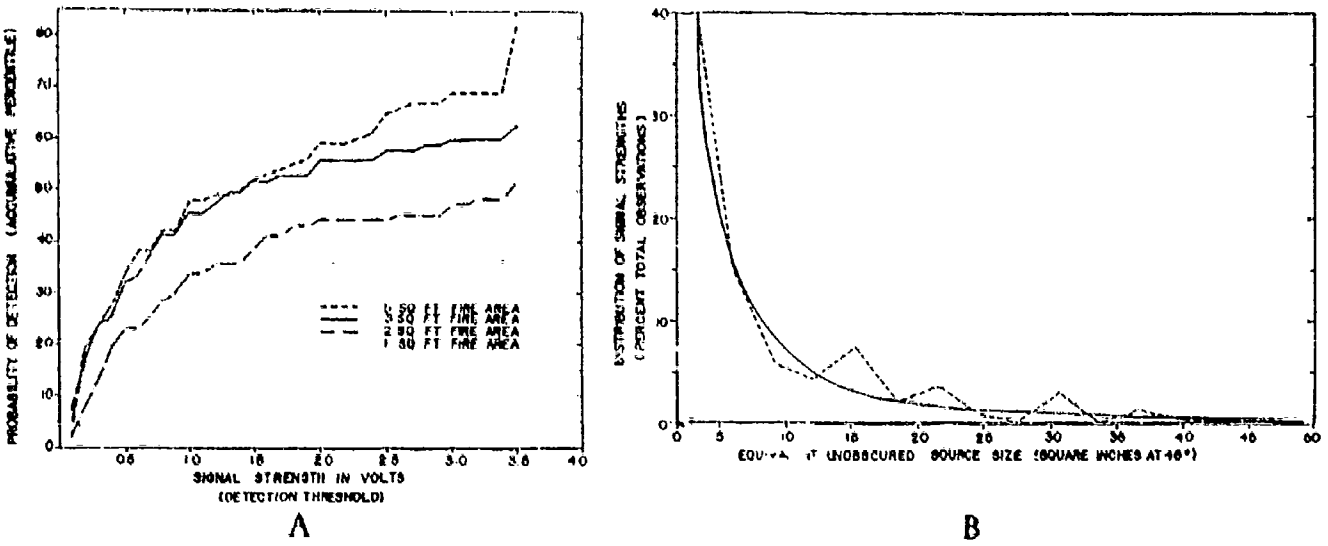

Figure 24 — *A*, Accumulative percent of total observations versus signal strengths for 1-, 2-, 3-, and 5-square-foot targets; *B*, frequency of occurrence of equivalent unobserved source sizes (1-square-foot targets at 45°).

effect that increased fire area has on detection probability. The accumulative percentage of signal strengths to total samples (i.e., percent detection versus detection voltage threshold) is shown in figure 24*A* for four sizes of fires: 1, 2, 3, and 5 square feet of fire area. The 1-, 2-, and 3-square-foot sources were buckets placed close together; the 5-square-foot source was the standard 5-bucket array on a 3-foot-radius circle.

Comparison of figures 24*A* and 21*A* will indicate the denseness of canopy obscurations: e.g., about 60 percent of the observations of 5-square-foot targets had unobscured areas smaller than 12 briquettes (0.25-square-foot) or were more than 95-percent obscured. The relative differences of the 1- to 2-square-foot, 2- to 3-square-foot, and 3- to 5-square-foot target curves suggest a measure of obscuration sizes and distribution. (The large number of very small signals indicates the desirability of improving scanner system sensitivity.) Note also that, relative to the calibration curve (fig. 21*A*), the 1-square-foot target (2.5 v.) does not increase its detection probability after showing through the canopy an emissive area of approximately 15 square inches (i.e., equivalent to about five briquettes). Figure 24*B* indicates the frequency of occurrence of equivalent unobscured canopy "hole" sizes (from all four fire sizes).

The large number of small signals indicates that the open transmission paths are generally very small. Photographs of the timber canopy support this observation (fig. 25). These high contrast photographs depict the nature of the timber canopy obscurations. The camera was tilted up 45°. The scanner is located near the center of each frame. The numbers in parentheses are ordinate and abscissa, respectively, of plot locations evenly spaced throughout the area. Figure 26 provides more detail of the canopy obscuration. These plot locations were selected as representative of the full range of observed signal strengths. The smaller details of the canopy obscurations correlate more closely with signal strength (see also fig. 23). The observations demonstrate the existence and significance of a large number of transmission paths of small cross sections associated with the small signals.

These observations establish the existence of a large number of relatively small signals near detection threshold levels. Cursory comparison of figures 21 through 26 shows the qualitative dependence of detection probability on (1) the canopy "hole" size and fre-

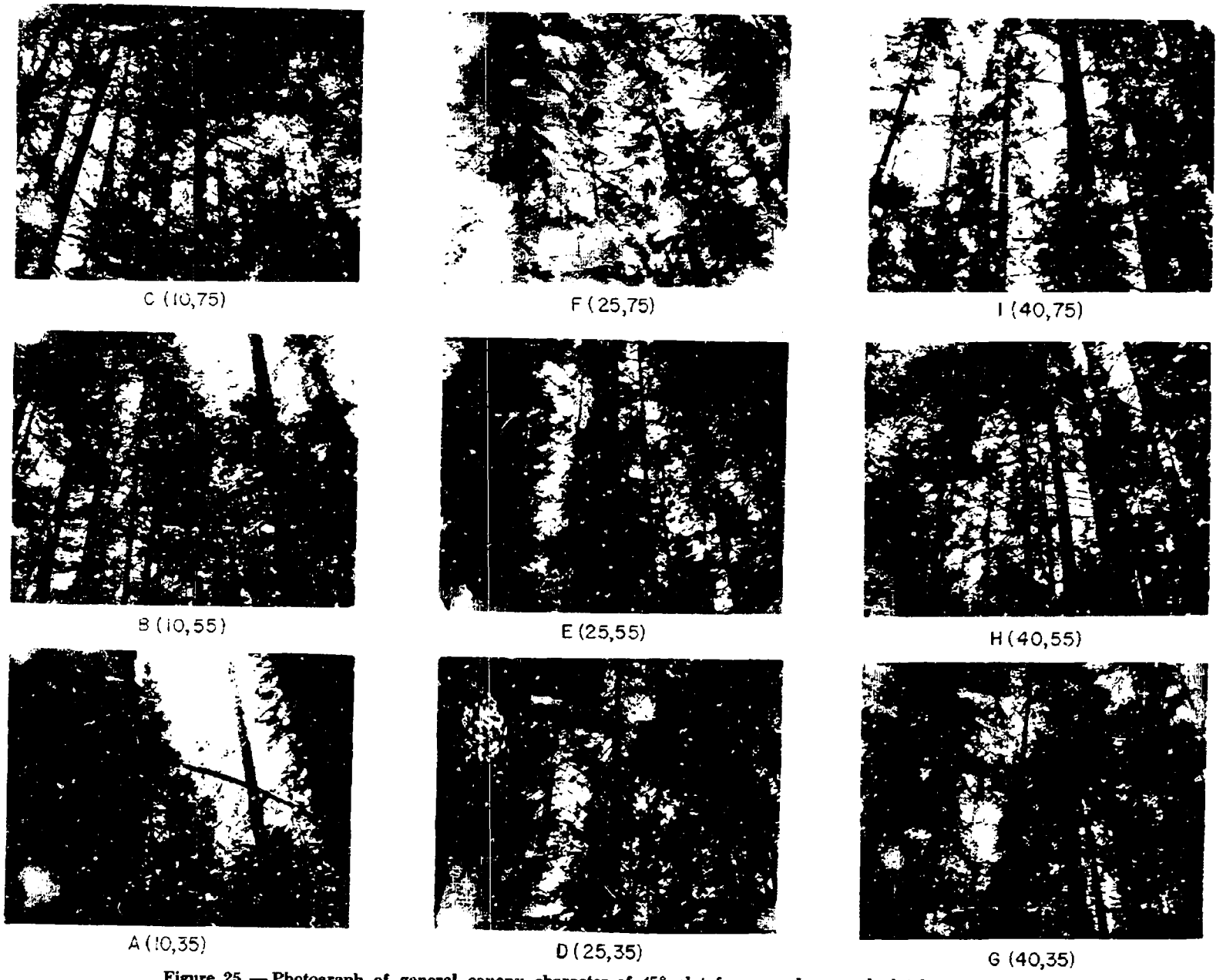

Figure 25. — Photograph of general canopy character of 45° plot from evenly spaced plot locations. Numbers in parentheses refer to plot location abscissa and ordinate associated with figures 22 and 23.

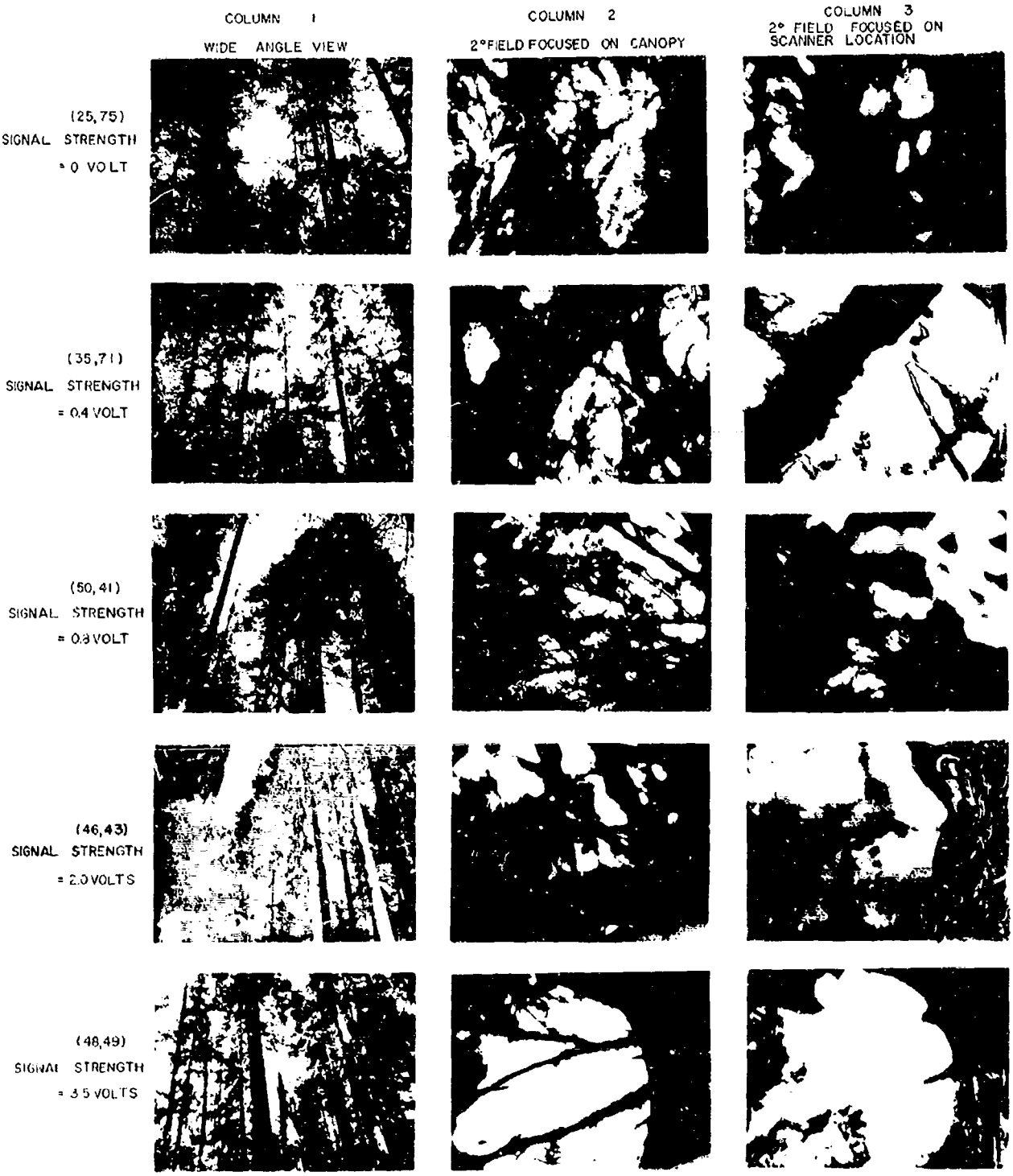

Figure 26. — Photograph of selected plot locations showing canopy characteristics associated with several values of signal strength.

quency of occurrence, and (2) the dispersion of trees throughout the timber stand.

It is inferred from these examinations that (1) a significant number of detections was accomplished with canopy obscurations as great as 90 to 95 percent, (2) the smaller transmission holes are distributed at about 1-foot intervals, and (3) the sizes of the large obscured areas and relatively unobscured areas roughly span a small (1 to 3) number of individual tree crowns.

A detection probability (i.e., percent positive observations) was calculated for the respective 1-, 2-, 3-, and 5-square-foot sources for 45° plot as follows:

Fire size (Square feet)	Percent detection (Percent)
1	37
2	51
3	63
5	82

The signal profile of figure 23, demonstrates the inhomogeneous distribution of positive detection reports. The question arises: 'Is the test plot (45 by 50 feet) large enough to be considered representative of the timber stand? Starting arbitrarily at the center of the plot, several square areas of increasing size were considered. In each of these areas the percentage of positive signals was noted and graphed. Percent detection has not yet stabilized when the limits of the plot edge are reached (fig. 27). Consideration of tree-shape factors (i.e., projected crown height/width ratio) and distribution of trees indicates that the plot should be approximately twice as deep (90 to 100 feet) and that the present width (50 feet) is sufficient for representative sampling.

Detection Predictions at 45° For Spot Fire Models

The detailed signal-obscuration profile of the 45° plot (fig. 23) provided the opportunity to examine the probability of detecting different model spot fires. By superimposing a template of a model fire on the signal profile of figure 23, detection was predicted by observing signals falling within the model.

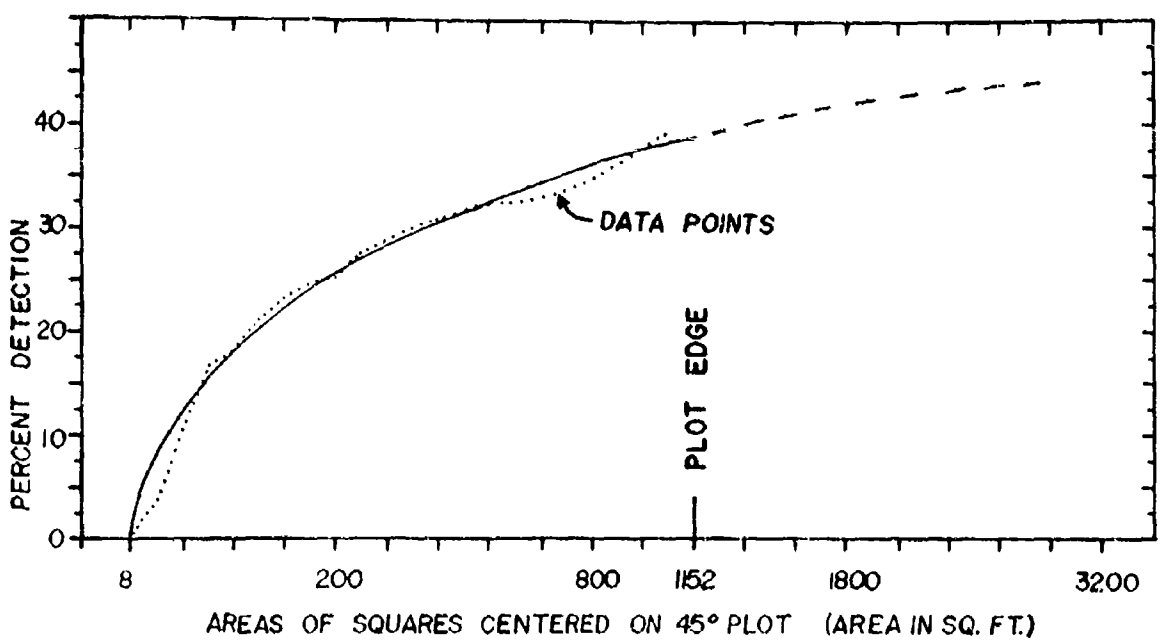

Figure 27. — Measured percent of positive detections as a function of increasing test plot size.

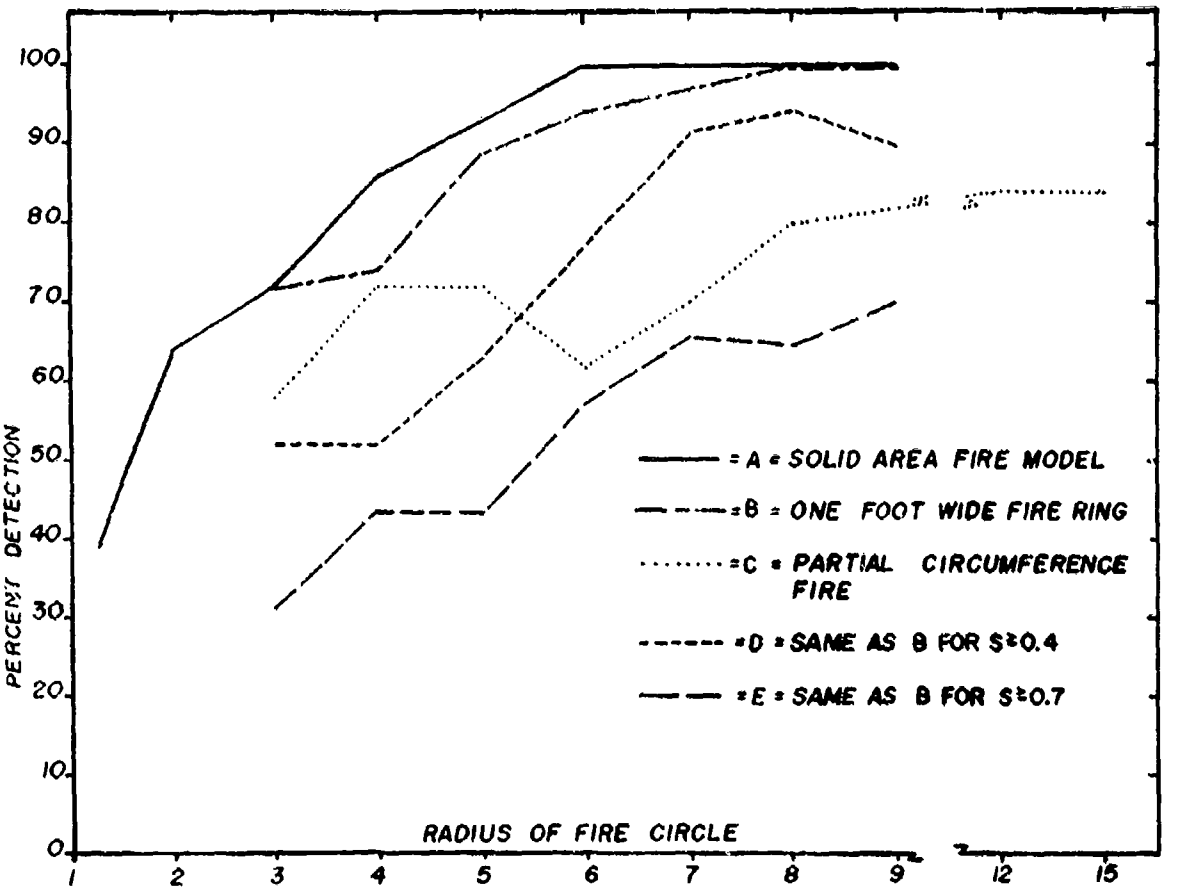

Figure 28. — Percent detection at 45° determined for three fire models as a function of model size and signal threshold.

Three fire model configurations were considered: (A) A solid burning circular area; (B) a 1-foot-wide circular burning ring; and (C) five 1-square-foot burning areas randomly spaced around a circle. The fire radius was varied for each model. Detection probability at 80 random plot locations for each configuration was evaluated as a function of "fire" radius. Positive detection was recorded when a positive scanner signal fell within the "burning" fire area. Results of this analysis are plotted in figure 28, curves A, B, and C. Also examined was the effect of increased detection signal threshold on the detection probability for the circular-ring fire (fig. 28, curves D and E). Qualitatively, these higher thresholds decreased the detection probability, as was expected.

The probability of detection does not increase significantly for fires larger than 9 feet in radius (fig. 28, curve C (the five-fire array)). This may indicate that 9 feet is the normal radius of influence of any tree or group of trees. This correlates nicely with inferences of the same effect observed from the flight data.

The distance to the nearest positive signal from each fire center was recorded (histogram, fig. 29). In no case was the fire center more than 5 feet from at least one positive signal. This indicates that a spot fire started anywhere under this canopy would become observable sometime before it had grown to a 5-foot radius.

Evaluation of the sum of signal intensities within each modeled burning area is usually a more reliable prediction of detection probability. These sums should then be examined with varying signal intensity detection thresh-

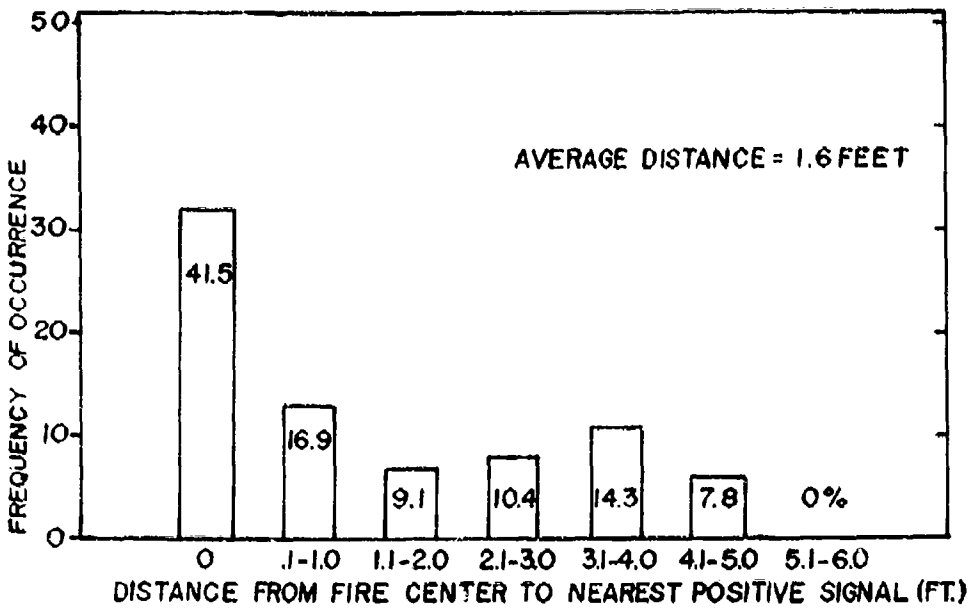

Figure 29. — Frequency distribution of distances from random locations to nearest positive detection.

olds. This evaluation will be one of the goals for experiment redesign. Accurate techniques for calibration and test area enlargement are required if the sampling is to be more representative of the timber stand.

Detection probability for the models is inherently low. The larger "burning" area of the models may have subtended several small transmission paths that would have added up to a positive detection report; however, these paths individually could have attenuated the 1-square-foot targets' transmitted intensity below the .1-volt detection threshold resulting in a negative detection prediction.

A rough evaluation was made to investigate the significance of integrating over several minute transmission paths. Although the radiation intensity from a single small transmission path may be below the level of detection threshold, the total radiation from several such paths may be great enough to give positive detection. While taking samples for fire model A (solid circular fire), each positive detection signal strength that fell within an individual "burning" area was recorded. Eighty random samples were taken of each fire size. The frequency of occurrence of signal strengths versus fire size is plotted in figure 30.

Several observations are worth noting. In each case, fewer than 1 percent of the signals were in the 2.5- to 3-volt interval. The percentage of signals stronger than 3 volts increases slowly with fire size. The distribution of small and intermediate signals tends to gather into fewer signal strength increments as fire size increases. And the mean signal strength of this group tends to larger values with larger fire size. From these observations we may conclude: (1) The total radiation from the smaller transmission paths (individually below system threshold) accounts for the dependence of detection probability on detection signal threshold, and (2) the smaller holes may be spatially distributed in a more homogeneous manner than the larger transmission paths.

Lack of adequate calibration and timber cruise measurements forces us to defer the rigorous statistical correlation of these parameters until more reliable data are produced.

Appendix V includes a brief discussion of theoretical approaches to timber canopy obscuration.

Detection Probability Beyond 45°

Measurements were made at 16 different angles beyond 45 vertical angle. The target

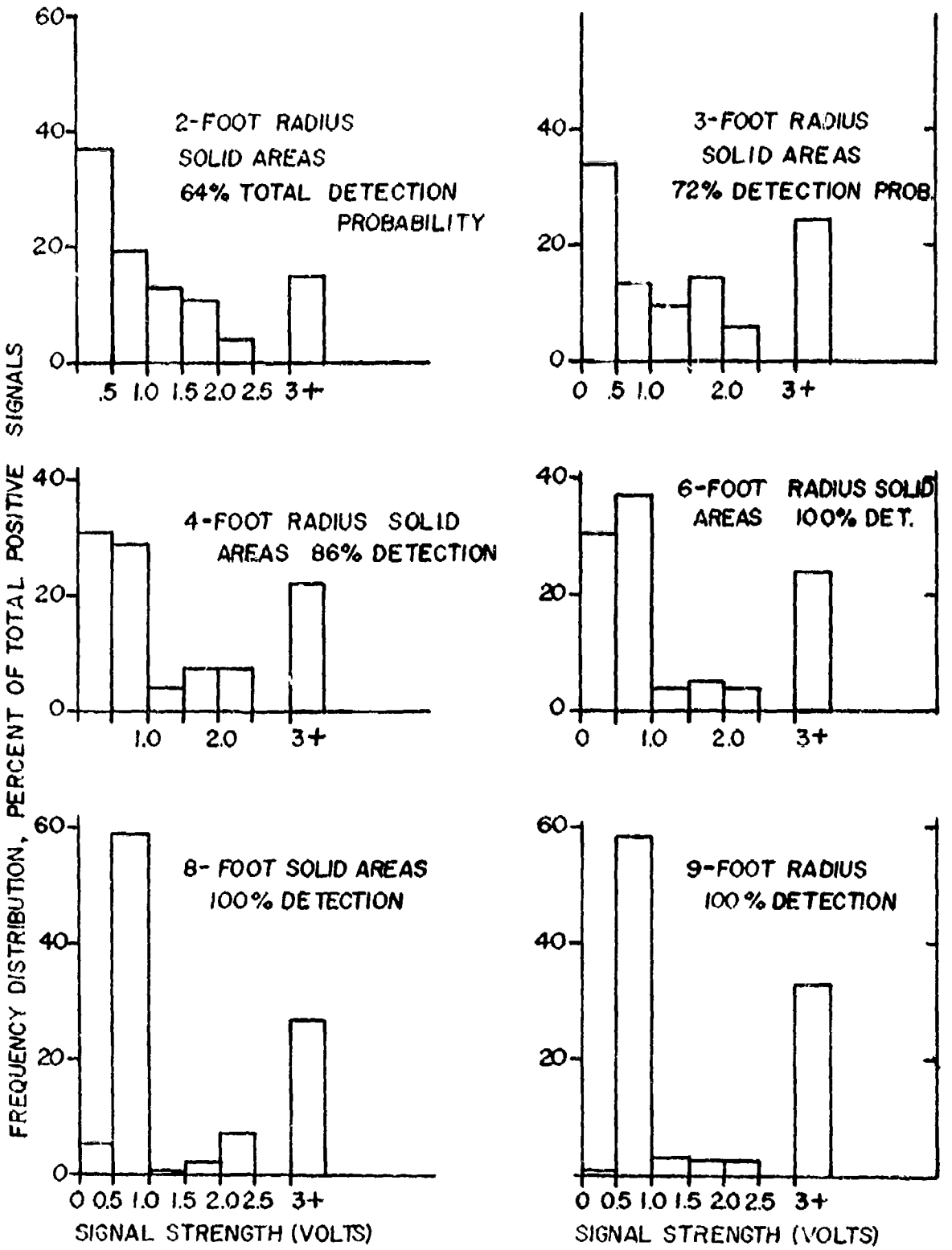

Figure 30. — Frequency distribution of signal strengths versus size of the solid fire model A.

array of five buckets on the 3-foot radius was used exclusively. A 1/16-square-foot signal bucket was used on each run for scanner orientation and calibration. Measurements of detection and signal strength were made at 50 random points along 100-foot lines at each scanner angle. Some of the gross variations may be explained by slope of terrain, species composition, and stand character, but it was not possible to normalize these data to obtain a smooth detection versus angle curve.

The angular dependence results are presented (fig. 31) as raw data; i.e., no attempt was made to normalize the individual points to average stand characteristics. At present we can only acknowledge that the points are very ragged.

After the detection data were taken, extensive timber cruise measurements were made on five representative lines. Stand density data were recorded adjacent to and in front of the five plots that showed the largest differences in percent detection. No correlations have been found between percent detection and any of the following: bole diameters, number of trees per acre, tree heights, basal area, crown weights, or arbitrary visual estimates of crown density. Two significant correlations were: (1) The greater the amount of larch or Douglas-fir present, the greater was percent detection, and (2) conversely, concentrations of Engelmann spruce, alpine fir, and grand fir tended to lower the detection probability.

The most prominent observable factors about the test lines were:

1. The 50° line had 10° favorable slope.
2. Measurements on the 61° line were

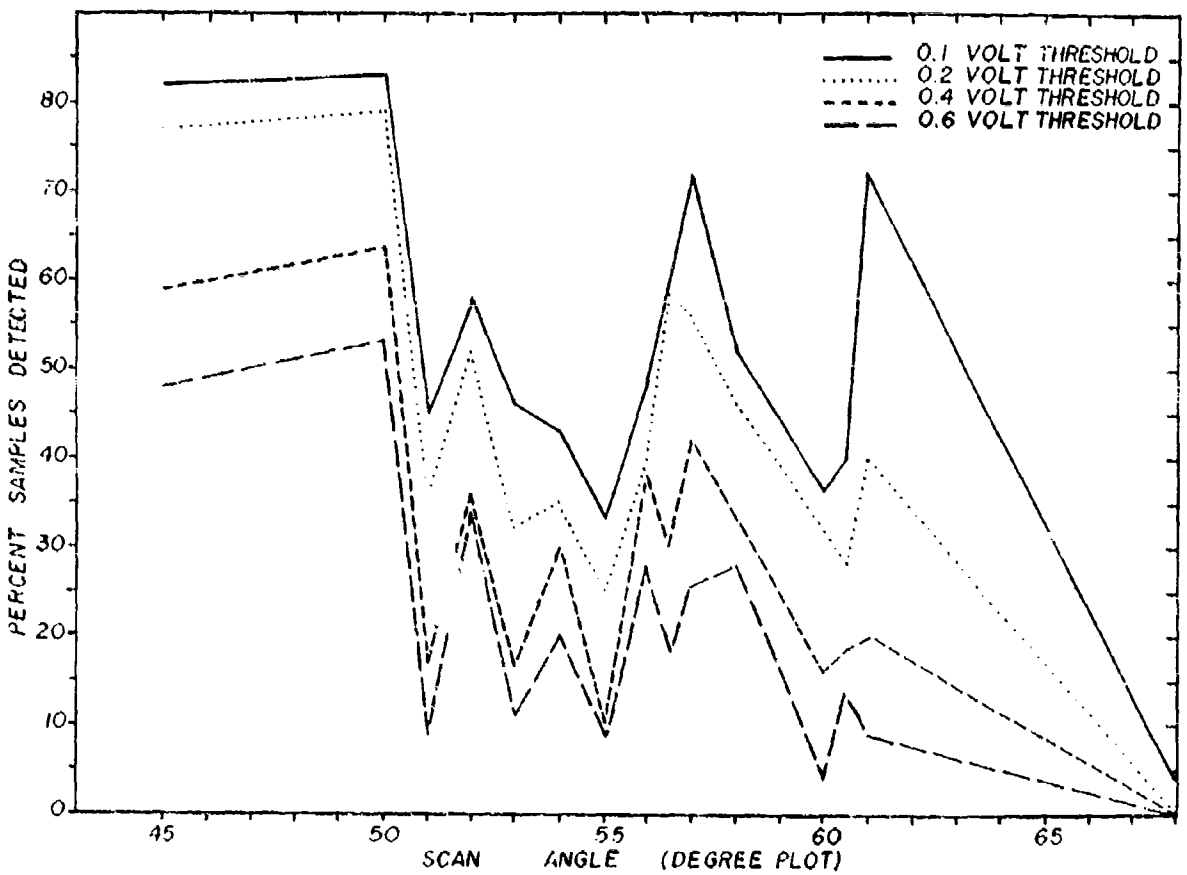

Figure 31. — Percent detection versus aspect angle for several detection signal thresholds.

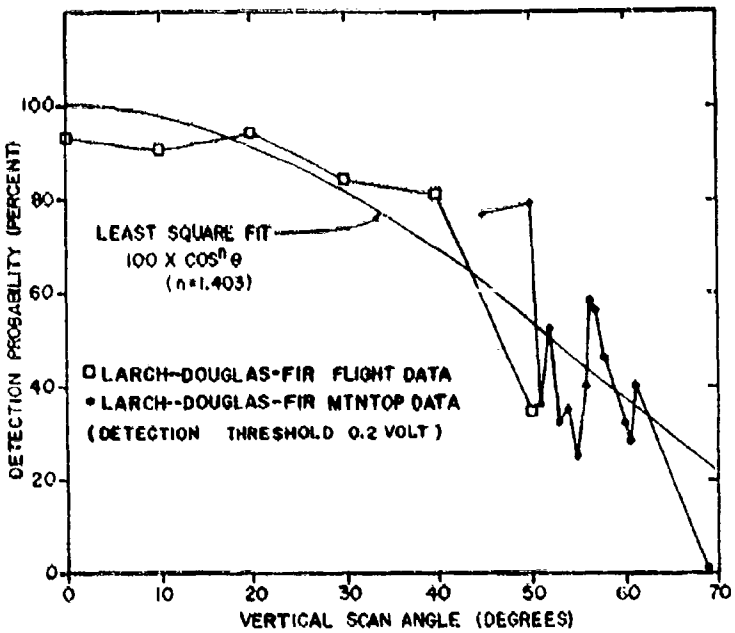

Figure 32.—Phase II, larch—Douglas-fir flight data to 50° extended past 60° by the mountaintop test data.

unique in that they were taken on a very windy night. Also, the timber was largely intolerant species (i.e., "easy site").

3. The 60° line was a short distance from the creek and had a dense understory of Pacific yew (*Taxus brevifolia* Nutt.) brush. Measurements made after this brush was removed increased detection from 10 to 36 percent.

4. Lines 60°, 60½°, and 61° were within a short distance of one another, progressing from wet ground near the creek toward a dry slope occupied by intolerant species.

However, foresters predicted that variation of detection probability would depend more on changes in angle around the 60° - 61° area than on differences in timber type. This is evidently not true. Most of the statistical ambiguities in the detection probability — timber cruise correlation can be attributed to inadequate sample size for the measurements.

In spite of the odd character of figure 31,

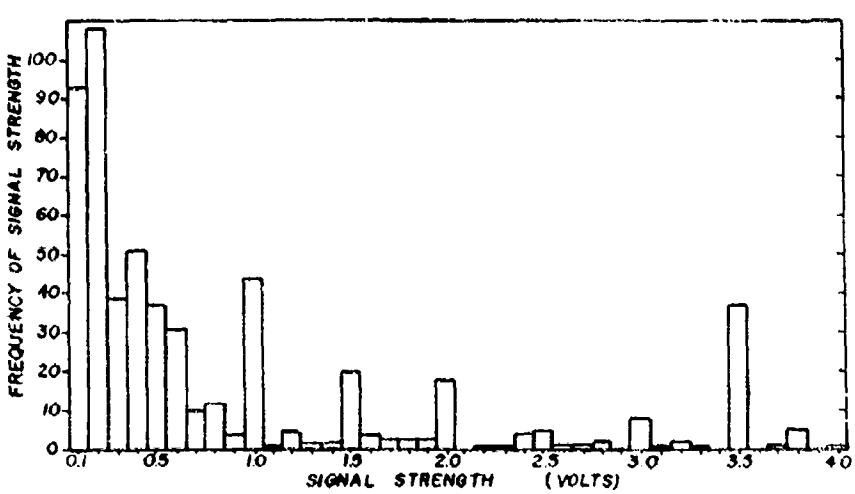

Figure 33.—Frequency of occurrence for all 5-square-foot target arrays, 45° to 69°, by signal strength.

there is no reason to expect that these measurements do not qualitatively describe the existing physical conditions.

To interpolate the detection probability versus aspect angle data between the one-look method of the flight program and the mountaintop test series, a detection criteria relationship between the two must be established. Targets observed on the flight imagery were detected when the target intensity exceeded the maximum background intensity. The criteria that mountaintop target signals must exceed the peak background signal (described in Appendix IV) established 0.2-volt as the appropriate detection threshold. When used as an extrapolation of the flight data (fig. 32), the mountaintop data look a little better.

Pursuant to geometric considerations discussed in Appendix IV, the best fit ($\cos^n\theta$) curve was adjusted to the data and statistically tested. The best fit, $n = 1.40$, gave an R.M.S. standard error of measurements of 13.3-percent error and an expected ±2.6-percent error at the 95-percent confidence level.

The frequency of occurrence of signal strengths for all data on the 3-foot-radius five fire arrays is shown in figure 33. It is interesting to note the test observer's personal preference for integral and half-integral voltage values. The relation between percent detection and mean signal strength at each of the test plots was examined with the Spearman Rank-Order (Rho) correlation coefficient, r. The resultant corrected correlation was $r = +.98$, or approximately a 1-to-1 relation between the two sets of measurements. This correlation is logical and has been assumed in the past; however, it had not been previously justified by rigorous argument.

The accumulative percent detection for successively larger detection signal thresholds is presented in table 4 for all data on 3-foot-radius fires, and in these angular increments: 45°, 50° to 54°, 55° to 59°, and 60° and greater. This was an attempt to smooth out the detection probability versus angle data and to examine the effects of higher detection threshold. The smoothing effect directly resulted from fewer but larger angle classes

Table 4. — Percent detection for various signal level thresholds, at aspect angles 45° to 60°

Detection signal threshold (Volts)	Aspect angle increment			
	45°	50° - 54°	55° - 59°	+60°
	Percent			
0.0	100	100	100	100
.1	82	55	53	40
.2	76	46	42	26
.3	60	35	34	16
.4	55	32	30	13
.5	49	25	26	9
1.0	43	24	21	6
1.5	28	12	11	1.5
2.0	23	9	7	1
2.5	22	6	4	
3.0	16	5.8	3	
3.5	14	5	2	

encompassing a greater number of measurement samples per class.

It appears, then, that about 300 to 500 individual measurements are necessary to establish a reliable detection probability in a given timber type at a given aspect angle.

Summary of Mountaintop Test Series

The original objectives of the mountaintop test have not yet been met. This test was planned as the first of a series of possibly two or three tests. The first effort was successful in that it yielded information about the relative value of several obscuration parameters.

Among the deficiencies are:

1. Sampling of percent detection versus angle was poor and inadequate. It is evident now that representative sampling will require test plots three to five times larger than those used. Up to 500 data samples per plot will be necessary.

2. The timber cruise measurements were inadequate for correlation with signal obscuration data.

3. Human bias in the recording of the data was obvious.

4. The limited dynamic range and nonlinearity of the electronic amplifiers introduced uncertainties into the data.

5. Calibration techniques were inadequate for reducing data to reliable absolute units.

The positive results of the test include:

1. The unique instrumentation requirements, logistics problems, and site preparation are now familiar.

2. The general trend of percent detection versus angle is established.

3. The cause and importance of the large number of very small signals have been identified.

The usefulness of five separate buckets in the standard test array has been questioned and discussed at length. The use of five separate sources in one target array does introduce N^3 times the minimum acceptable number of unknowns in any detection probability equation; e.g., five separate measurements of a single bucket "should" more precisely measure detection probability. With a five-bucket array, one does not know which bucket is obscured and which is producing a positive detection signal.

Results of the first mountaintop effort should be regarded as inconclusive. However, these results will be reviewed continually as criteria for experimental design for the continuation of the program.

CONCLUSION

SUMMARY OF PHASES I, II, AND III

During the 3 years of the development and field evaluation of an infrared detection system, many limiting factors have been identified, equipment has been produced to overcome some of the limitations, and some data have been generated on which feasibility can be judged. Except in situations where the patrol area is small and well defined, the usefulness of daytime patrol is limited. The probability of detecting small fire targets as a function of flight pathwidth in four representative timber types is qualitatively defined. For detection purposes the four species tested are in two classes as follows: (1) "easy" detection class, including larch—Douglas-fir, lodgepole pine, and ponderosa pine; and (2) "difficult" detection class, Engelmann spruce.

Operational feasibility of an infrared fire patrol system ultimately is judged on its capability for detection under various measurable conditions of forest and terrain. Instrumentation used to measure any phenomenon must have sufficient sensitivity. A state-of-the-art system is necessary in order that the effects of silva and topology on detection can be determined. The scanning system now in use is not adequate for this purpose. More sophisticated discrimination techniques are needed if the low-intensity signals from timber-obscured targets at angles beyond 50° are to be detected reliably.

Comparison of high altitude imagery with aerial photographs appears to give accurate description of fire location. The Convair T-29 aircraft, equipped with the Doppler radar navigation system, has the capability to follow patrol corridors accurately during nighttime detection flights. The moving window display provides immediate readout of information with high resolution.

The research capability developed during this period undoubtedly will prove to be the most significant contribution toward the operational development of the airborne infrared detection system. The project now has a staff experienced in infrared techniques and qualified to develop and test a superior system.

PLANS FOR THE FUTURE

Design criteria based on detection criteria discussed in Appendixes III and IV have been written for the construction of an infrared receiver and electronic video system to meet the specific requirements of the Fire Scan research program. This system will include a seven-channel tape recorder. A taped video record of detection experiments will allow signal strengths, background temperature difference, and background frequency characteristics to be examined in the laboratory. These are needed to adequately quantify the system's capability.

The 1965 flight program will evaluate this state-of-the-art scanning system. Prior to the test program, the Convair T-29 aircraft will undergo an IRAN inspection and the Doppler system will be inspected and repaired. Experiment design and acquiring adequate instrumentation will be emphasized.

APPENDIX

		Page
I	DESCRIPTION OF TEST AREA	38
II	CRITERIA FOR SPECTRAL RESPONSIVITY	42
III	SENSITIVITY OF SCANNING SYSTEM	44
IV	CRITERIA FOR DETECTION	46
V	ATTENUATION OF RADIATION	50

APPENDIX I

DESCRIPTION OF TEST AREA

Lodgepole Pine Test Area

1. *Test area designation and location.* — The area, within a very dense lodgepole pine stand, is located on the east side of Gold Creek approximately 6¼ miles north of State Highway 20. This area is on the Missoula Ranger District, Lolo National Forest. Legal description is S½SW¼ sec. 6, N½NW¼ sec. 7, T. 14 N., R. 16 W., PMM.

2. *Elevation and topography.*—The area, situated on a bench with low ridges and minor draws, has an elevation of 4,200 feet m.s.l. A marsh is on the east side toward the northern extremity. No slopes on the area exceed 20 percent.

3. *Timber type and size class.* — Timber consists of a typical stand of stagnated lodgepole pine (*Pinus contorta* Dougl.). Some young ponderosa pine (*Pinus ponderosa* Laws.) sawtimber grows on the northeastern portion of the area. The larch (*Larix occidentalis* Nutt.) — Douglas-fir (*Pseudotsuga menziesii* var. *glauca* (Beissn.) Franco) timber type borders the south and east edges of the test area. Density of the lodgepole pine is fairly uniform throughout. Basal area on the plots ranges from 0 in small openings within the stand to 227 square feet per acre.

4. *Direction of flight paths.* — Flights over the area are due north and south; true azimuths, 0° to 180°.

5. *Cruise summary.* — Number of plots in area — 50; acreage of test area — 34.44 acres (1,000 feet by 1,500 feet); prism basal area factor — 20.

Ponderosa Pine Test Area

1. *Test area designation and location.* — The area, within a medium density ponderosa

Table 5. — Cruise information from lodgepole pine test area

Timber measurements	Test area		
	Lodgepole pine	Ponderosa pine	Average or total
Trees per acre	156	5.2	161.2
Net volume per acre (b.f.)[1]	8,730	320	9,050
Average basal area per tree (sq. ft.)	.57	1.02	.795
Average d.b.h. (inches), weighted	10	14	10.1
Average tree height (feet), weighted	62	53	61.7
Average lower crown limit, both species in mixed stand (feet)	—	—	28
Average crown thickness (feet), both species	—	—	44
Cumulative stem density, d.b.h. X trees in each diameter class (inches)	—	—	2,662
Crown cover density (percent) as estimated by aerial photos over test fire areas	—	—	80

[1]*Scribner log rule was used for all merchantable volumes. Cruise includes all merchantable trees 8 inches d.b.h. and larger (by 2-inch classes).*

pine stand, is located on a bench south of the Big Blackfoot River, approximately 1 mile west of State Highway 20. The NE¼ sec. 35, T. 14 N., R. 15 W., PMM, encompasses the area. This area is on the Lubrecht Experimental Forest, University of Montana.

2. *Elevation and topography.* — Elevation of the area is 3,650 feet m.s.l. Terrain is slightly rolling, with no slopes more than 10 percent.

3. *Timber type and size class.* — Timber on the area is a stand of residual ponderosa pine. Patches of stagnated pole stands are scattered throughout the area. Average height of dominant and codominant trees in the area of young, thrifty, mature timber is 58 feet, while in the areas of reproduction the average height is 12 feet, consisting of about 80-percent total crown. Density of the ponderosa pine increases toward the south side of the test area (slope with a north aspect) where it becomes intermingled with Douglas-fir. As the slope with a north aspect increases in gradient to 30 percent, the pine decreases to scattered clumps in a predominantly Douglas-fir stand. Basal area for plots ranged from 0 to 190 square feet per acre; the less dense plots were on the north side of the area. Average basal area for the overall test area was 73 square feet per acre.

4. *Direction of flight paths.* — Flight paths run due east and west; true azimuths, 90° and 270°.

5. *Cruise summary.* — Number of plots in test area — 70; acreage within area — 34.44 acres; prism basal area factor — 10.

Larch — Douglas-Fir Test Area

1. *Test area designation and location.* — The area, located within a medium density

Table 6. — Cruise information from ponderosa pine test area

Timber measurements	Test area		
	Ponderosa pine	Larch - Douglas-fir	Average or total
Trees per acre	67	0.1	67.1
Net volume per acre (b.f.)[1]	5,316	13	5,330
Average basal area per tree (sq. ft.)	1.14	1.06	1.13
Average d.b.h. (inches), weighted	14.5	14	14.5
Average tree height (feet), weighted	58	60	58.1
Average lower crown limit, both species in mixed stand (feet)	—	—	18
Average crown thickness (feet), both species	—	—	40
Cumulative crown density, all plots (inches)	6,540	82	6,622
Apparent crown cover density (percent) from aerial photos over test fire areas	—	—	60

[1]*Scribner log rule was used for all merchantable volumes. Cruise includes all merchantable trees 8 inches d.b.h. and larger (by 2-inch classes).*

larch—Douglas-fir stand, is approximately 1¼ miles east of State Highway 31, and 1½ miles north of Pierce Lake. This area is on the Condon Ranger District, Flathead National Forest. An approximate legal description is: NE¼ or SW¼ sec. 10, T. 19 N., R. 16 W., PMM.

2. *Elevation and topography.* — Elevation of the area is 4,500 feet m.s.l. Terrain is moderately rolling slopes.

3. *Timber type and size class.* — Timber on the area is old-growth Douglas-fir and larch. The sparse reproduction is predominantly Douglas-fir, an average of 40 feet high and almost 100-percent total crown height. Density of the timber (stems per acre) is uniform over the entire area, varying only in species composition. Basal area for the 50 plots ranged from 20 square feet to 260 square feet; average overall basal area was 149 square feet per acre.

4. *Direction of flight paths.* — Flight paths run north and south; true azimuths, 0° and 180°.

5. *Cruise summary.* — Number of plots on test area — 50; acreage of timber within area — 34.44 acres; prism basal area factor — 20.

Table 7. — Cruise information from the larch - Douglas-fir test area

Timber measurements	Test area				
	Douglas-fir	Lodgepole pine	Engelmann spruce - alpine fir	Larch	Average or total
Trees per acre	71.1	14.9	11.0	23.8	120.8
Net volume per acre (b.f.)[1]	8,168	1,316	1,800	5,639	16,923
Average basal area per tree (sq. ft.)	1.20	.69	1.25	1.73	1.21
Average d.b.h. (inches), weighted	15	11	15	17	14.9
Average tree height (feet), weighted	75	77	80	97	82
Average lower crown limit, all species in mixed stand (feet)	—	—	—	—	35
Average crown thickness (feet), all species	—	—	—	—	47
Cumulative stem density, all plots (inches)	2,656	238	450	1,536	2,224
Apparent crown cover density (percent) from aerial photos over test areas	—	—	—	—	80

[1]*Scribner log rule was used for all merchantable volumes. Cruise includes all merchantable trees 8 inches d.b.h. and larger (by 2-inch classes).*

Engelmann Spruce — Alpine Fir Test Area

1. *Test area designation and location.* — The area, within a heavy density Engelmann spruce—alpine fir stand, is located on a plateau about 2 miles southeast of Skookum Butte Lookout. This area is on the Powell Ranger District, Clearwater National Forest. Legal description of the area is the SW¼ sec. 7, T. 38 N., R. 22 W., BM.

2. *Elevation and topography.* — Elevation of the area is 5,800 feet m.s.l. Terrain is slightly rolling with no slopes more than 10 percent.

3. *Timber type and size class.* — Timber on the area consists of a stand of overmature Engelmann spruce with scattered grand fir and alpine fir in association. The average height of dominant and codominant trees in the area is 98 feet. Basal areas for the plots ranged from 120 to 360 square feet per acre, while the average basal area for the entire test area was 225 square feet per acre.

4. *Direction of flight paths.* — Flight paths run north and south; true azimuths, 0° and 180°.

5. *Cruise summary.* — Number of plots in test area — 50; acreage within area — 34.44 acres; prism basal area factor — 20.

Table 8. — **Cruise information from the Engelmann spruce - alpine fir test area**

Timber measurements	Test area				
	Larch - Douglas-fir	Grand fir	Alpine fir	Engelmann spruce	Average or total
Trees per acre	0.7	6.3	20.7	133.0	160
Net volume per acre (b.f.)[1]	63	1,621	3,841	35,864	41,208
Average basal area per tree (sq. ft.)	1.48	1.74	1.47	1.71	1.6
Average d.b.h. (inches), weighted	16.5	18	16.5	18	17.5
Average tree height (feet), weighted	48	83	82	88	86
Average lower crown limit (feet), all species in mixed stand	—	—	—	—	23
Average crown thickness (feet), all species	—	—	—	—	62
Cumulative stem density (inches), all plots	—	—	—	—	10,344
Crown cover density (percent) from aerial photos over test areas	—	—	—	—	100

[1]*Scribner log rule was used for all merchantable volumes. Cruise includes all merchantable trees 8 inches d.b.h. and larger (by 2-inch classes).*

APPENDIX II

CRITERIA FOR SPECTRAL RESPONSIVITY

Since the advent of solid state semiconductor technology, new devices have been developed that provide capabilities for measurement, at high speed and low intensity levels, of the low energy electromagnetic radiation associated with infrared (IR) wavelengths.

A review of typical sources of radiation and infrared detector responsivities is necessary to establish criteria for system design pertinent to our special applications.

Of immediate interest to the Forest Service is the application of techniques of infrared remote sensing to forest fire surveillance. Here three possible sources of infrared radiation exist — the radiant emission of the fire itself, the emission from terrain background, and the interference of illumination from sources such as the sun.

The spectral radiant emission of real world emitters is measured by their deviation from a theoretically defined ideal black body radiation source. The emissive powers at several black body source temperatures are shown in figure 34. Glowing, burning fuels associated with applications in forest fire surveillance closely approximate the ideal black body radiation curves. In the 3- to 6-micron region, typical terrain background emitters may fall 15- to 20-percent below the theoretical curves, but generally stay within 90 percent of the emission expected from a true black body.[10] Also shown is the spectral irradiance of the sun[11] and rough indications of the transparent atmospheric windows.

To facilitate system design, first the optimum spectral wavelength region is selected, and it in turn is dependent on the nature of the phenomenon to be observed.

Fire surveillance requires not only that burning fuels be detected, but also that their location relative to observable terrain background features be determined. Small spot fires are most easily detected in the spectral region where the fires are most intense (2 to 7 microns, fig. 34). Similarly, terrain background detail is best acquired near the peak of the ambient black body curve (5 to 20 microns).[12] Very little information is available concerning the reflectance of solar radiation from terrain in the intermediate and far infrared regions. The solar spectral irradiance for zero atmospheric absorption (fig. 34) can be used as an upper bound for the expected interference from sunlight. Both terrain reflectance and atmospheric absorption attenuate the reflected sunlight intensity. A spectral wavelength region should be selected as far from the solar irradiance peak as practicable; in this application, this must be to the longer wavelength side. Also very significant, the spectral bandpass must overlap an atmospheric transmission window.

In general, the following qualitative deductions can be made:

1. Thermal emissive temperatures of terrain background can best be measured in the 8- to 14-micron atmospheric window; however, significant information can be acquired in the 3- to 4.2-micron and 4.5- to 5.3-micron windows.
2. Glowing fuel beds can be detected best against a terrain background in the 2- to 2.6-micron, 3- to 4.2-micron, and 4.5- to 5.3-micron windows.
3. For daytime fire detection, the 2- to 2.6-micron band, and possibly the lower part

[10] *Fredrickson, W. R., N. Ginsburg, and R. Paulson Infrared spectral emissivity of terrain. Final Rep. Syracuse Univ. Res. Inst., ASTIA Doc. No. AD 155552, WADC - TR - 58 - 2229. 153 pp., illus. 1958.*

[11] *U.S. Air Force. Handbook of geophysics. Rev. ed. New York: Macmillan. 656 pp., illus. 1961.*

[12] *U.S. Air Force Cambridge Res. Lab. (Max Nagel, ed.). Background measurements during the infrared measuring program. 1956. Geophysics Res. Dir., ORD Res. Note 46, AFCRL - TN - 60 - 692.*

of the 3- to 4.2-micron band, must be rejected because of reflected solar irradiance.

Considering the above deductions, the use of the 3- to 4.2-micron and preferably the 4.5- to 5.3-micron bands is justified. The Fire Scan program has confirmed these observations in practice; hence, further rigorous theoretical treatment is not now necessary.

A cursory examination of sensitivity parameters of available infrared detectors shows that photoconductive and photovoltaic indium antimonide (InSb) detectors have the most outstanding characteristics in the spectral range of interest to this test. These devices are photoelectric transducers, which supply the electric signal to the electronic video chain. Within their proper dynamic range, the electrical output signal is proportional to the infrared radiant intensity measured in the focal plane of appropriate optical collectors.

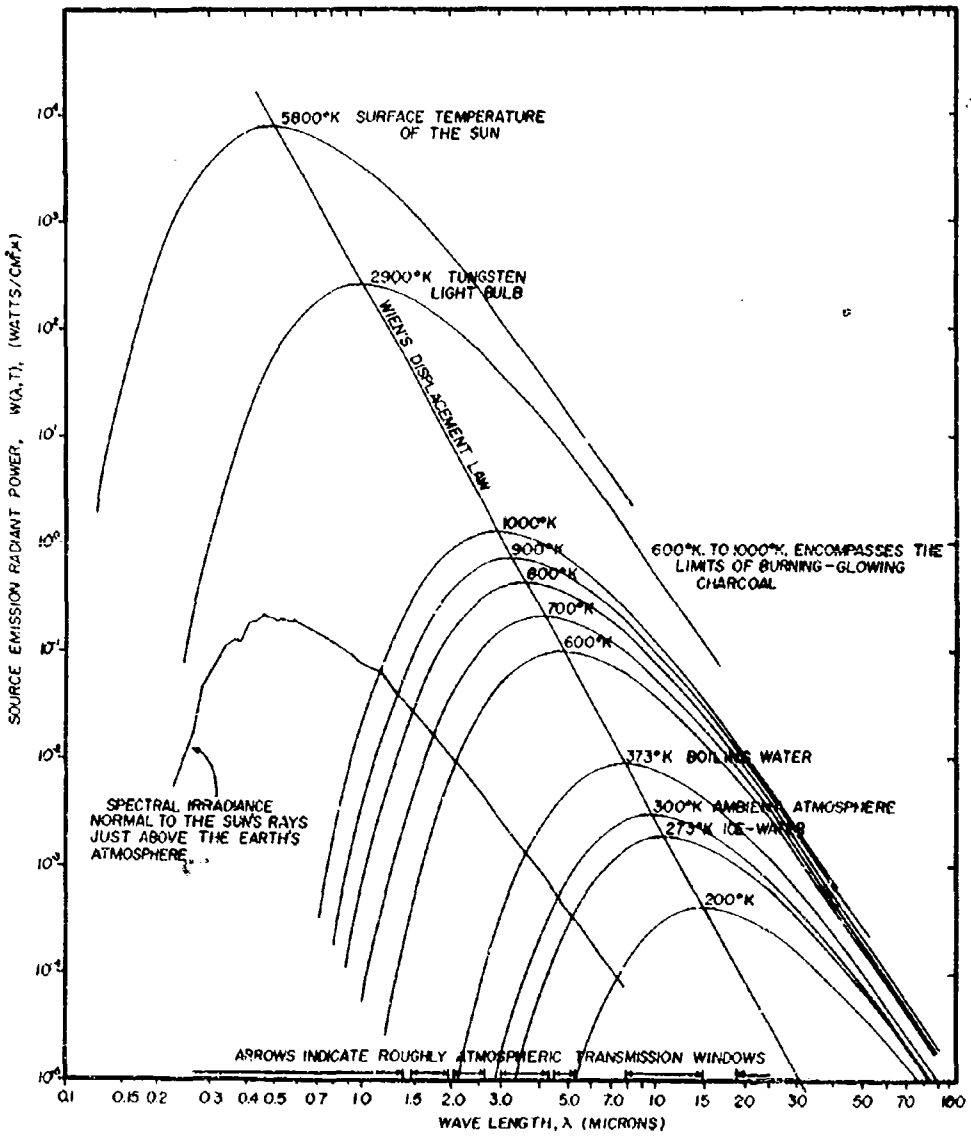

Figure 34. — Absolute spectral emissive powers for black bodies at various temperatures.

APPENDIX III

SENSITIVITY OF SCANNING SYSTEM

Remote sensing devices usually collect radiation with modified Newtonian or Cassigrainian telescopic systems. The detectors measure the total radiation falling on them at some point in the optical image plane. To compare the large number of individual points over an extended terrain object plane and thus provide the relative spatial information, an optical-mechanical scanning mechanism must be provided. This is accomplished by placing a spinning, flat mirror in front of the collector objective. On an aircraft platform, the infrared optical receiver is oriented so that the spinning mirror looks down and scans abeam of the aircraft from one side to the other. The velocity of the aircraft allows TV-like scanning of the two-dimensional object plane (see fig. 35, Appendix IV, scanning instrumentation and geometry).

The radiant power, E, reaching the detector is the product of the power density, $\frac{1}{\pi} W(\lambda,T)$, from the source; the solid angle, ω, subtended by the source from the receiver; and the area, A, of the optical collector objective:

$$E = \frac{1}{\pi} W(\lambda,T) \cdot A \cdot \omega$$

For easy calculation, the Stephan-Boltzman equation is used to estimate $W(\lambda,T)$ for total output power of the source. Then, the power, E, is modified by some constant, k, which is the fraction of the total power that is included by the system spectral sensitivity. Calculation of k is made by numerical integration over empirical measurements of the system spectral response (fig. 39, Appendix V).

The Stephan-Boltzman law states:

$$W = \epsilon\sigma T^4$$

Where ϵ is the emissivity of the source, σ is the constant of proportionality, $\sigma = 5.67$ watts cm.$^{-2}$deg^{-4}, and T is the absolute temperature in degrees Kelvin. Then E becomes,

$$E = \frac{k}{\pi} A\omega\epsilon\sigma T^4.$$

The term for temperature resolution in the limit of small temperature differences:

$$\Delta E = \frac{4k}{\pi} A\omega\epsilon\sigma T^3 \, \Delta T.$$

Solving for ΔT,

$$\Delta T = \frac{\pi \Delta E}{4A\omega\epsilon k\sigma T^3} \qquad \text{Eqn. 1}$$

The infrared detector detectivities, D^*, are defined by

$$D^* = \frac{S/N}{J} \sqrt{a\Delta f} \qquad \text{Eqn. 2}$$

where S/N is the signal to noise voltage ratio measured for a specific detector irradiated by power, J; a is the detector area; and Δf is the electrical frequency bandwidth used in the detectivity measurement.

By definition:

$$E = J, \text{ when } S/N = 1 \qquad \text{Eqn. 3}$$

Combining equations 1, 2, and 3 now redefines ΔT as the noise equivalent temperature (NET):

$$NET = \Delta T = \frac{\pi \sqrt{a\Delta f}}{4D^* A \omega\epsilon k\sigma T^3} \qquad \text{Eqn. 4}$$

This equation is further refined by examining $\sqrt{a\Delta f}$ in terms of system parameters.

The area of the detector, a, defines the field of view or resolution element from optical principles as:

$$a = F^2 \omega$$

where F is the focal length of the objective, which has area A.

Further, Δf is the rate at which the terrain field is covered, divided by the optical resolution element:

$$\Delta f = \frac{2\pi \; V/H \text{ (steradians/sec.)}}{\omega \text{ steradians}}$$

Then equation 4 becomes:

$$NET = \frac{F\left(\frac{\pi^3}{8} \cdot \frac{V}{H}\right)^{1/2}}{D^* k\, \epsilon\sigma\, T^3 A\, \omega}$$

where:

F = focal length of collection optics.

V/H = velocity to height (altitude) ratio, to be specified by performance requirements (V/H of .2 or .4 steradian/sec. is typical).

D^* = broad band detectivity of detector; typically, 2×10^{10} watts^{-1}cm.sec.$^{-1/2}$.

$\epsilon(\lambda)$ = spectral emissivity of background.

k = percent total spectral power of the source accepted by system, for parameters of figure 39, Appendix V; $k = 0.071$ when atmospheric spectral windows are accounted for.

σ = Stephan-Boltzman constant, 5.67×10^{-12} watts cm.$^{-2}$deg.$^{-4}$.

T = background average temperature, °K.

A = area of optical collector objective.

ω = optical system resolution, steradians.

Typical NET's are of the order of 1°K. to 2°K. for ambient terrain background with systems using the 3- to 6-micron spectral range.

APPENDIX IV

CRITERIA FOR DETECTION

The electrical signal (video) processing chain in infrared line scanners generally is not d.c. coupled. Hence, an absolute radiometric background intensity reference level is not maintained. However, the background radiation intensity does fluctuate about some local mean value. This mean intensity level shifts relative to the clamped output d.c. signal level over large terrain distances, but does not significantly change over small distances. A system's response to these gross changes is fixed by its scanning speed and low frequency cutoff. For the remainder of this section we shall assume the video system has sufficiently wide bandwidth to establish a short-term d.c. signal level associated with the local mean background radiant intensity.

This kind of equipment is sufficiently sensitive to map terrain background. Accurate detection of hot targets against a terrain background depends upon radiometric criteria.

Define the following terms:

T_0, T_1, T_2, T_3	Temperatures (°K.) of local mean background, coolest point and warmest point in background, and hot target, respectively.
$\omega = \delta^2$	Instantaneous field of view.
A	Area of target.
K	Target signal to background signal ratio (explicitly defined below).
$N(\lambda,T)$	Spectral radiance (watts/steradian cm.^{2} micron).
$W(\lambda,T) = \pi N(\lambda,T)$	Spectral radiant emittance (watts/cm.^{2} micron).
θ	Aspect angle (see fig. 35).
r	Slant range.
h	Altitude.
D	Total scan width.
$R(\lambda)$	Responsivity of scanning system (volts/watt, i.e., watts incident on unit square aperture of scanner).
S	Scanner output signal (volts).
a	Area of scanner aperture.

The signal from the system is related to source radiation by:

$$S(T) = a\omega_0 \int^{\infty} R(\lambda)\, N(\lambda,T)\, d\lambda.$$

Since $R(\lambda)$ is not an analytic function, this calculation is made by numerical methods, e.g.:

$$S(T_i) = \sum_j a\omega R(\lambda_j)\, N(\lambda_j,T_i)\ \Delta\lambda_j.$$

Consider a target much smaller than the instantaneous field of view with no obstruction or attentuation in the optical path. Figure 36 is a typical scanner video output signal. S_0 is the clamped d.c. signal bias. Define S_1 and S_2 as signal levels from the coldest and warmest (T_1 and T_2) spots, respectively, in the neighborhood of the momentary field of view and S_3 as the signal from a particular field that contains a hot target to be detected. Let $(S-S_0)$ be the dynamic signal that is proportional to the variation of radiant intensity about the local mean radiant intensity,

$$\omega[N(\lambda,T) - N(\lambda,T_0)]\ \Delta\lambda.$$

Unless complex signal discrimination is used, in order for a small target to be "detectable" the signal from the spot, ω, containing the target must be greater by some factor, K, than the signal from the warmest spot in the background. From figure 36 this becomes:

$$S_3 - S_0 \geq K(S_2 - S_0). \qquad \text{Eqn. 5}$$

For targets much smaller than ω, the worst case, as shown in figure 36, occurs when the target is situated in the coolest spot in the background.

S_3 then becomes:

$$S_3 = \int_{\lambda=0}^{\infty} a\, R(\lambda) \left[\frac{A \cos\theta}{r^2} N(\lambda,T_3) + \left(\omega - \frac{A}{r^2}\right) N(\lambda,T_1) \right] d\lambda.$$

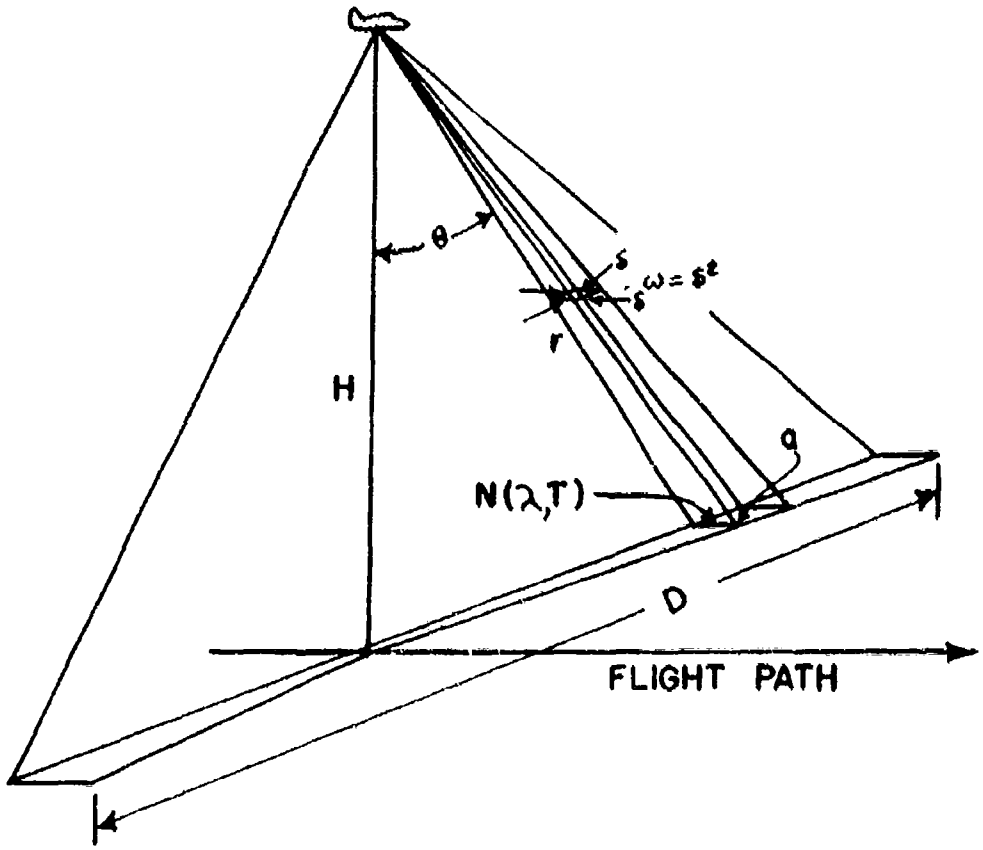

Figure 35. — Aircraft scanning geometry.

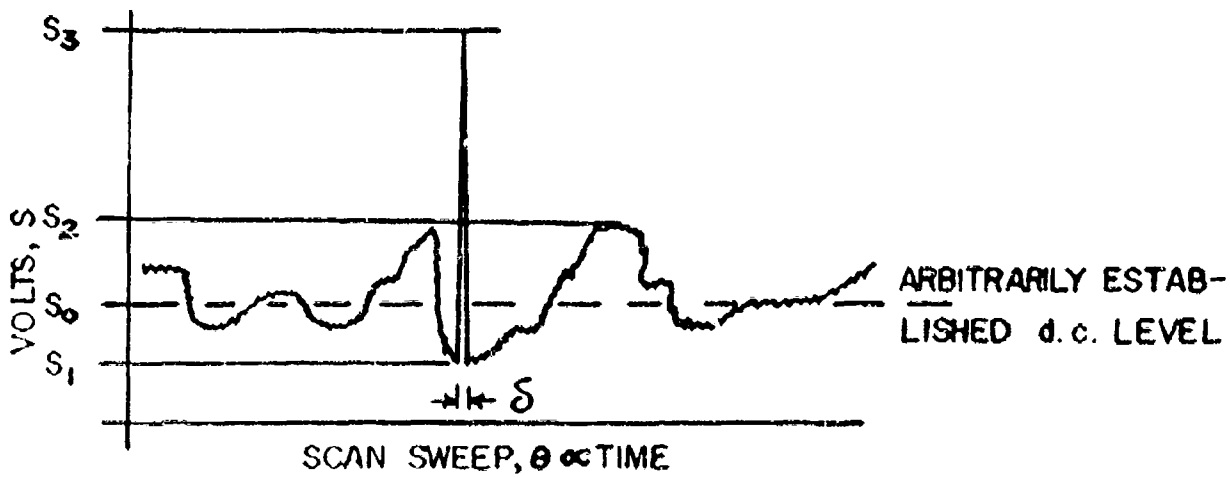

Figure 36. — Typical video signal oscilloscope trace.

Since T varies with θ, S_0 is determined by:

$$S_0 = \frac{a\omega}{\theta_2-\theta_1}\int_{\lambda=0}^{\omega} R(\lambda) \int_{\theta_1}^{\theta_2} N(\lambda,T)\, d\theta d\lambda.$$

where θ_1 and θ_2 are defined such that:

$$(\theta_2-\theta_1) \geq \frac{1}{f}\frac{d\theta}{dt}$$

where f is low frequency limit of system bandpass, and $\frac{d\theta}{dt}$ is the scanning speed. To be more precise, S_0 is determined by the preset system d.c. bias. This calculation determines the associated T_0 or $S(T_0)$ in the neighborhood of $\theta_1 < \theta < \theta_2$.

Define S_T as the signal from target alone and assume

$$\omega >> A/r^2.$$

Then:

$$S_1 = S_T + S_1.$$

Criteria for detection then becomes:

$$S_T \geq K(S_2-S_0) + (S_0+S_1) \qquad \text{Eqn. 6}$$

S_0, by definition, is the mean signal level, approximately one-half way between S_1 and S_2 (fig. 36).

Hence:

$$S_2-S_0 \approx S_0-S_1 \approx \frac{S_2-S_1}{2}.$$

Thus, we can define a new K' greater than 1 such that Eqn. 6 becomes:

$$S_T \geq K'\left(\frac{S_2-S_1}{2}\right)+\left(\frac{S_2-S_1}{2}\right)$$

or

$$S_T \geq (K'+1)\left(\frac{S_2-S_1}{2}\right) \qquad \text{Eqn. 7}$$

$$S_T = a\,R(\lambda)\,\frac{A\,\mathrm{Cos}\,\theta}{r^2}\,N(\lambda,T_3) \geq (K'+1)\,\frac{a\,R(\lambda)}{2}\,\omega[N(\lambda,T_2) - N(\lambda,T_1)]$$

$$\frac{A\,\mathrm{Cos}\,\theta\,N(\lambda,T_3)}{r^2} \geq (K'+1)\,\frac{\omega}{2}\,[N(\lambda,T_2) - N(\lambda,T_1)]$$

$$\frac{A}{r^2} \geq \frac{(K'+1)}{\mathrm{Cos}\,\theta}\,\frac{\omega}{2}\left(\frac{N(\lambda,T_2) - N(\lambda,T_1)}{N(\lambda,T_3)}\right) \qquad \text{Eqn. 8}$$

A note should be made here about instrumentation. The system readout has been assumed to be a signal display (fig. 36) presented by a C.R.T. Large or very intense target sources give adequate signatures for detection. The marginal sources are the ones of concern and are usually much smaller than the instantaneous field, ω.

Electronic detection by pulse-height discrimination (P.H.D.) is much more precise than visual interpretation. The upper trace of figure 37 shows the capability of a typical narrow-band, pulse-height discriminator to distinguish a low amplitude "spike" target signal from large variations in the background intensity as is shown in the lower trace of the same figure. Since the small targets are the major problem, we suppose that the P.H.D. should be narrow banded about the field sampling frequency, f, such that:

$$f = \frac{1}{\delta}\frac{d\theta}{dt}$$

With the narrow-band provision, the lower limit on S_T could be decreased since the ter-

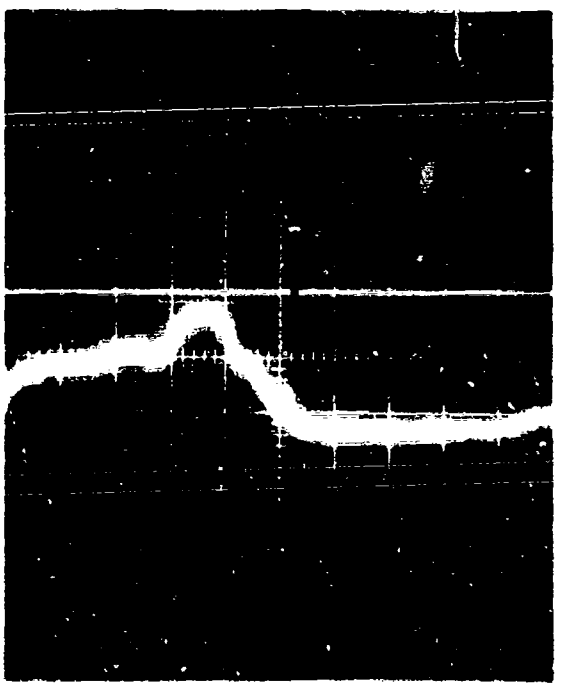

Figure 37. — Pulse-height discrimination circuit separating low amplitude, high frequency signal from background.

rain background features are generally much larger than the instantaneous field, δ^2. Detection of smaller values of S_T would, however, involve a significant increase in the false alarm rate. If a certain false alarm rate is not objectionable, the absolute lower limit of S_T is determined by the system noise level, n_s.

$$S_T \geq n_s$$

and

$$\frac{a A \operatorname{Cos} \theta \, N(\lambda, T_3) \, \Delta\lambda}{2\delta^2} \geq NET.$$

Note it is meaningless to talk in terms of K in this narrow-band limit since S_0, S_1, S_2, etc., are not established.

Referring again to Eqn. 8:

$$\frac{A}{r^2} \geq \frac{(K'+1)}{\operatorname{Cos} \theta} \frac{\omega}{2}\left(\frac{N(\lambda, T_2) - N(\lambda, T_1)}{N(\lambda, T_3)}\right) \quad \text{Eqn. 8}$$

Let us assume that with appropriate instrumentation (P.H.D., etc.) we can reliably let $K' = 1$. Also, let $\theta = 0$, $T_3 = 800°K.$, $\omega = 10^{-6}$ steradians, and assume spectral bandwidth of 4.5 microns to 5.5 microns. Note that $h = r \operatorname{Cos} \theta$, $W(\lambda, T) = \pi N(\lambda, T)$, and $\Delta W = (W(\lambda, T_2) - W(\lambda, T_1))$.

Then Eqn. 8 reduces to:

$$\frac{A}{h^2} \geq 10^{-6}\left(\frac{\Delta W}{0.33 \text{ (watts/cm.}^2)}\right) = 3 \times 10^{-6} \, \Delta W. \quad \text{Eqn. 9}$$

Figure 38 shows a plot of A/h^2 against $\Delta T = T_2 - T_1$ for background temperatures (T_1 and T_2) around 300° K. ambient. It assumes (1) the detection criteria of equation 7; (2) that optical transmission losses do not bury any signals in the system noise; and (3) there is no target obscuration and you are looking straight down into the bucket.

The angular dependence of A/h^2,

$$\left(\text{i.e., } \frac{A}{h^2} \propto \frac{1}{\operatorname{Cos}^3 \theta}, \text{ where } r = h/\operatorname{Cos} \theta\right)$$

is a consequence of inverse square law and the Lambertian angular dependence on target radiant intensity. It is assumed here that the major terrain features are larger than the instantaneous field of view; hence, the terrain background signal is not attenuated by either of these features by the same factor as the small fire targets. When the target becomes larger than the instantaneous field of view, the angular dependence of detection criteria disappears and A/h^2 is independent of θ.

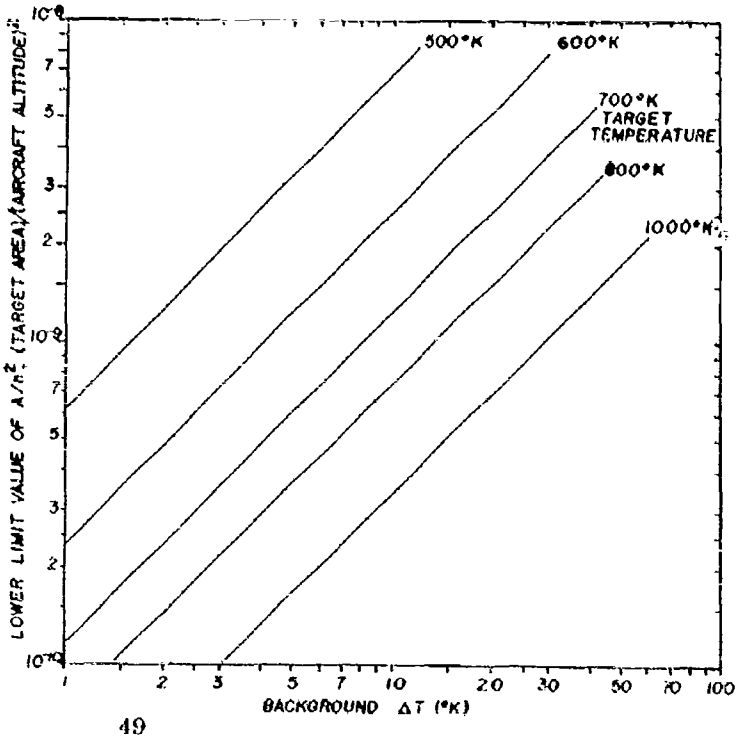

Figure 38—Lower limit values of (target area)/(aircraft altitude)² ratio as function of peak-to-peak background temperature variation for several target temperatures, assuming detection criteria of Eqn. 7 in the text.

APPENDIX V

ATTENUATION OF RADIATION

The radiation that reaches an airborne infrared scanner from a small incipient spot fire must traverse several attenuating media before it reaches the infrared detector. These media are of three basic types: (1) The geometric obscuration by tree boles, timber canopy, understory, and brush; (2) the atmospheric path consisting of molecular absorption mainly by H_2O and CO_2 and scattering by haze (smog, fog, smoke): and (3) the transmission character of the infrared receiver optics. The latter two media are spectrally dependent; we are discussing them in reverse order.

Infrared Receiver Transmission

The scanning mode is most easily accomplished by a rotating 45° mirror (high speed, nodding optical systems have prohibitive inertia).

The objective element also should be a mirror. Mirror objectives have only one optical surface to figure, have adequate resolution over small fields, and have no chromatic aberrations. However, these mirror objectives usually require at least one secondary folding mirror. Infrared lenses in general have good resolution over a larger field, but have very high reflection and transmission losses. Correction of chromatic aberration requires at least two elements; this requires the figuring of at least four optical surfaces. The relatively large apertures required make lenses both economically and technically prohibitive for the present application.

Mirrors are not perfect reflectors. A typical aluminized mirror has a reflectivity, $R = .92$ at 4 microns; silver and gold have higher reflectivities but are not as durable as an aluminized mirror. Hence, we can consider the optical transmission, T_{op}, of an aluminized mirror collecting system as:

1. A three-surface system:
   $T_{op} = (.92)^3 = .78$
2. A four-surface system:
   $T_{op} = (.92)^4 = .716$

The sensitivity of the infrared receiver is also governed by the spectral response of the detector and the spectral bandpass of the optical filter, if one is used. These are not conducive to analytic representation and, hence, must be handled by graphic or numerical integration. Typical detector and filter spectral curves are shown in figure 39.

Atmospheric absorption is a major concern in fire detection. The scattering effects are easily described. Smog and smoke particles associated with forest fires are much smaller than the Rayleigh limit for 3-micron radiation; so they are negligible in the present application. Indeed, very good terrain imagery has been obtained through smoke palls 2,000 feet deep. However, water condensate associated with clouds and fog renders them totally opaque. Therefore, we may consider the "scattering" transmission either:

$$T_{scat} = \begin{cases} 1, & \text{(smoke, smog)} \\ 0, & \text{(fog, clouds).} \end{cases}$$

Transmission of the Atmosphere

The problem of molecular absorption is more complex. The spectral region of interest (3- to 6-micron) contains significant H_2O and CO_2 absorption bands. Figure 40[13] shows typical atmosphere transmission. Figures 41 and 42 (U.S. Air Force)[14] show, respectively, H_2O and CO_2 transmissions. Since H_2O and CO_2 concentrations vary independently in the real world, they are handled analytically by separate absorption coefficients. CO_2 concentration is sufficiently stable in time that we consider only its variation with altitude (fig. 43). H_2O concentrations can be meas-

[13] *Yates, H. W. and J. H. Taylor. Infrared transmission of the atmosphere. U.S. Naval Res. Lab. Rpt. 5453. 1960.*
[14] *U.S. Air Force.* Op. cit.

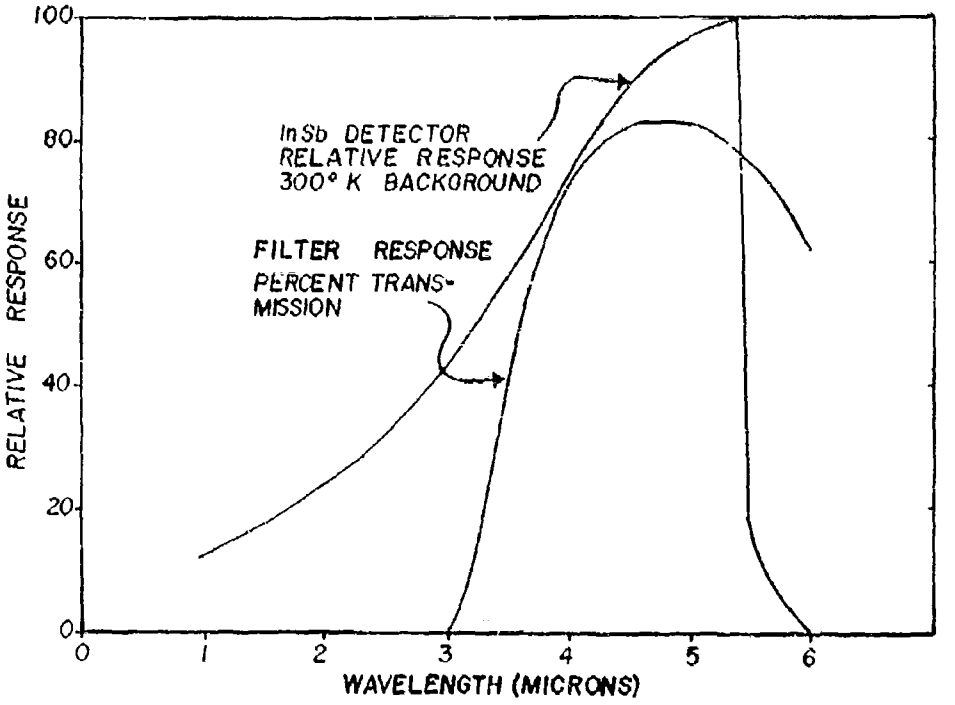

Figure 39. — Spectral characteristics of a typical detector and filter.

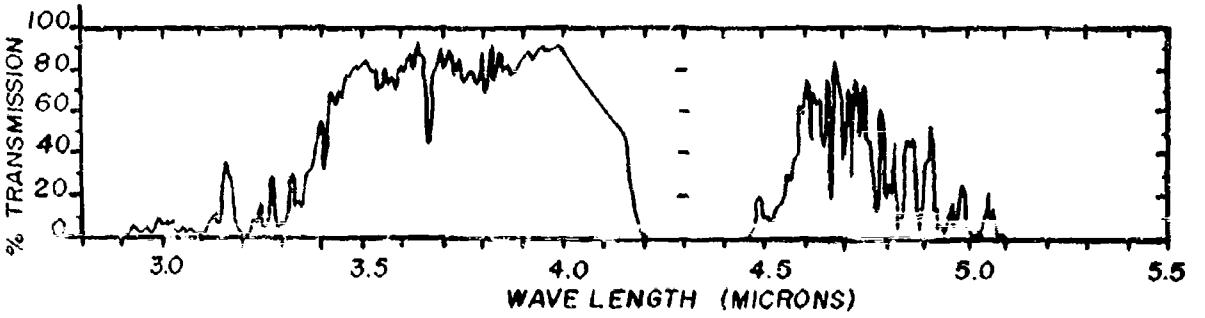

Figure 40. — Typical atmospheric transmission curve; 16.25 km. sea level path, 68.7° F., 53-percent relative humidity, 15.1 cm. H_2O in path.

ured by the relative humidity and dry bulb temperatures (fig. 44), and percent transmission estimated from figure 45. A cursory look at figures 44 and 45 proves that major changes in the minimum detectable signal level can be attributed to realistic variations of relative humidity.

Atmospheric transmission, particularly high H_2O concentration, is obviously one of the major parameters of significance to fire detection probabilities, and its effects should not be neglected.

Whenever possible, the practical procedure would be to use a known source, N_0 (λ,T) for system calibration.

If we have a linear system:

$$S = \frac{S_0}{N_0(\lambda,T)\ \Delta\lambda}\ N(\lambda,T)\ \Delta\lambda$$

Good practice requires calibration for several source intensities spread over the full dynamic range of the system.

Timber Canopy Obscurations

From the mountaintop test procedures described elsewhere in this report, qualitative conclusions were established concerning canopy obscuration factors. These may be separated into two types: first, the larger obscurations (almost always large tree boles), which

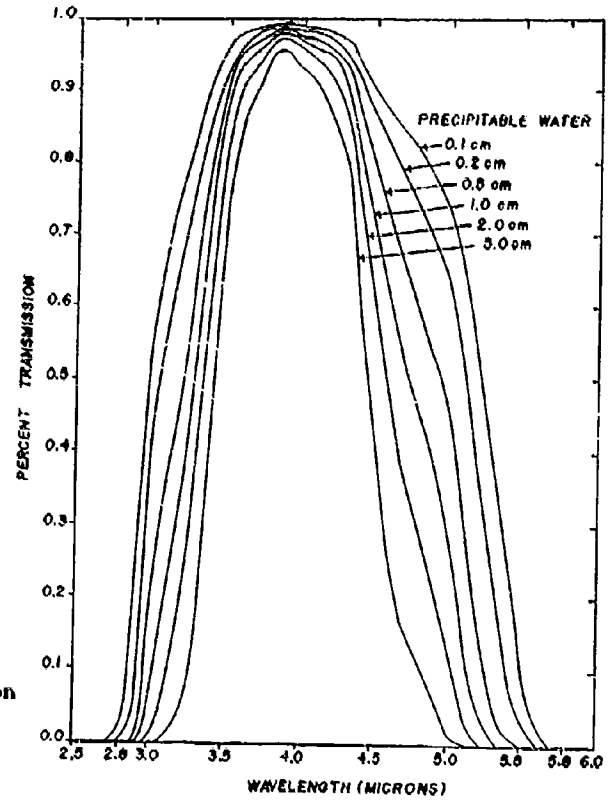

Figure 41.—Spectral transmission of water for various optical paths.

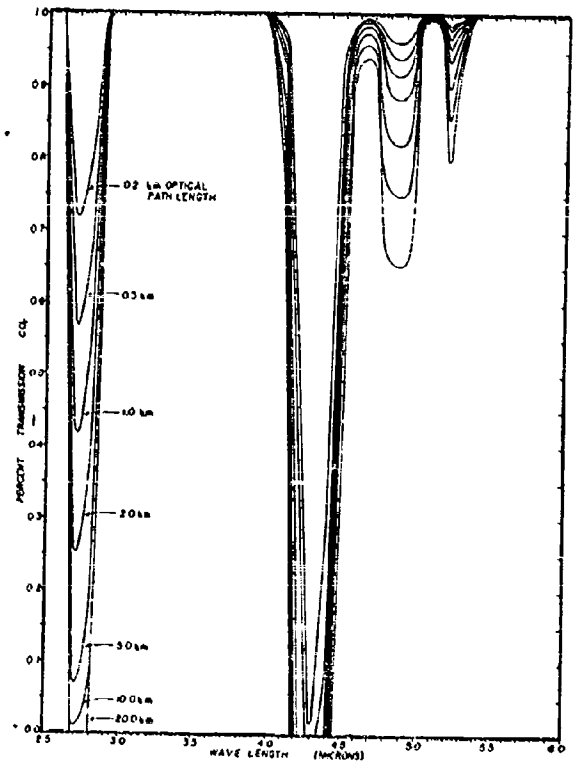

Figure 42.—Spectral transmission of CO_2 for various optical paths.

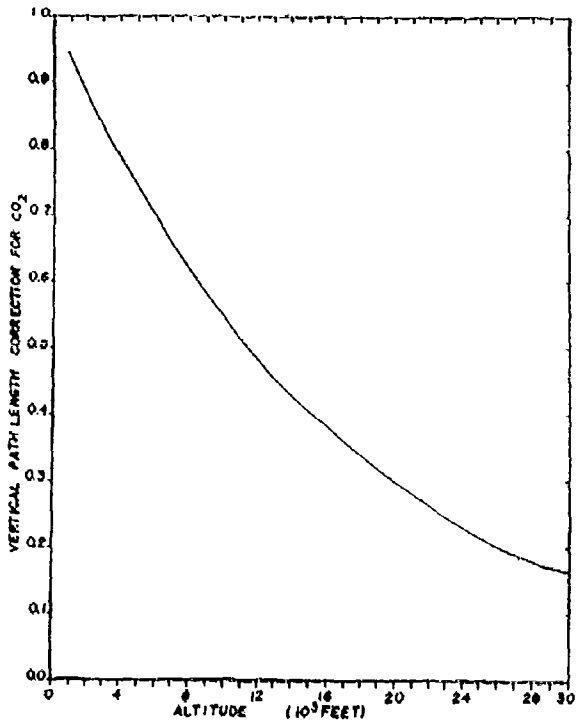

Figure 43.—Variation in atmospheric CO_2 concentration with altitude normalized to sea level.

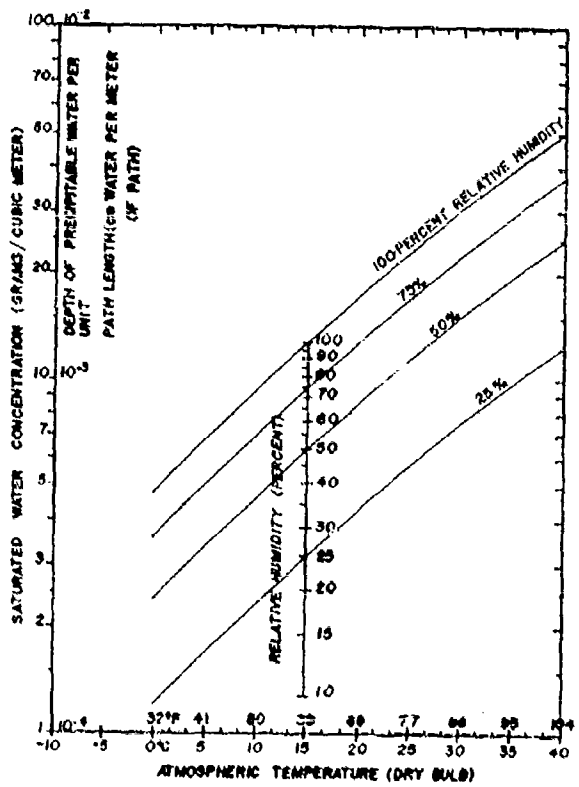

Figure 44.—Precipitable H_2O concentration as a function of atmospheric temperature and relative humidity.

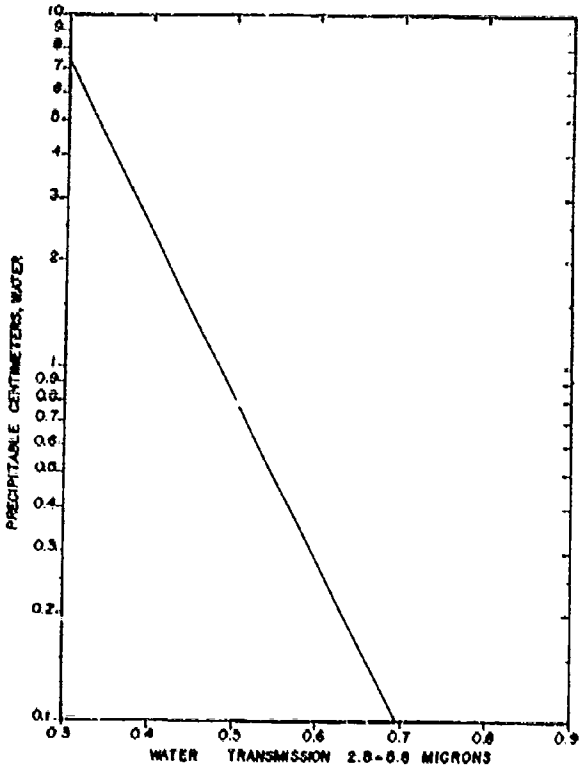

Figure 45.—Percent transmission of water in the 2.8-5.8-micron band versus concentration of precipitable water.

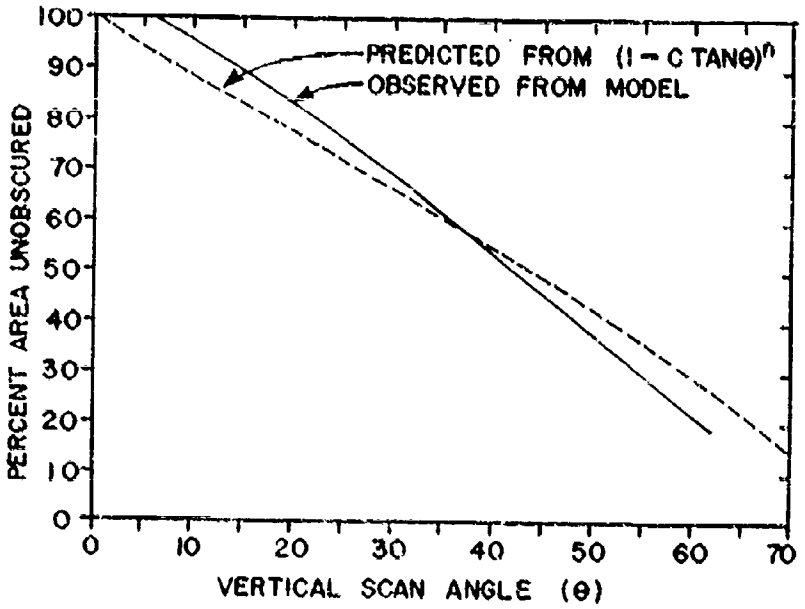

Figure 46.—Observed and predicted obscurations from a tree bole model.

totally obscured the targets; and, second, the small needle and limb obscurations, which only partially attenuated the target radiation.

A conifer tree bole can be approximated by an inverted parabaloid of revolution whose vertical cross sectional area is two-thirds its base diameter, d times its height h. The projected ground area obscured from an aspect angle, θ, is then:

$$\frac{2}{3} dh \operatorname{Tan} \theta$$

The percent unobscured area, ϕ_n, for a random stand of such tree boles becomes:

$$\phi_n = \left(1 - \frac{2/3\, dh \operatorname{Tan} \theta}{43{,}500}\right)^n$$

where d and h are measurements in feet, and n is the number of trees per acre. We tested this bole obscuration by constructing a model of a random tree stand and correlating actual measurements on the model with the formula prediction; results are plotted in figure 46. The model had equivalent timber cruise parameters of 328 square feet per acre basal area, (d.b.h.) of 1-foot and 82.2-foot tree heights.

A similar effort to relate obscuration to timber cruise parameters for the canopy overstory is contemplated. Since correlation of this type of attenuation with present timber measurements is lacking, a test to check any theory is unavailable. However, by the nature and distribution of signal strengths from the mountaintop tests, the following theoretical attenuation model is contemplated for the tree crowns:

$$\phi_x = \phi_0 e^{-\delta x}$$

where δ is related to crown characteristics and x is the optical path length, i.e.:

$$x = \frac{h}{\operatorname{Cos} \theta}$$

where h = crown depth, and θ = aspect angle as before. Further field measurements should provide data for correlation checks on these proposed relations.

The ultimate objective of these considerations is to provide field management personnel with a measure of the usefulness of remote sensing equipment in particular forested areas.

totally obscured the targets; and, second, the small needle and limb obscurations, which only partially attenuated the target radiation.

A conifer tree bole can be approximated by an inverted parabaloid of revolution whose vertical cross sectional area is two-thirds its base diameter, d times its height h. The projected ground area obscured from an aspect angle, θ, is then:

$$\frac{2}{3} dh \operatorname{Tan} \theta$$

The percent unobscured area, ϕ_n, for a random stand of such tree boles becomes:

$$\phi_n = \left(1 - \frac{2/3\, dh \operatorname{Tan} \theta}{43{,}500}\right)^n$$

where d and h are measurements in feet, and n is the number of trees per acre. We tested this bole obscuration by constructing a model of a random tree stand and correlating actual measurements on the model with the formula prediction; results are plotted in figure 46. The model had equivalent timber cruise parameters of 328 square feet per acre basal area, (d.b.h.) of 1-foot and 82.2-foot tree heights.

A similar effort to relate obscuration to timber cruise parameters for the canopy overstory is contemplated. Since correlation of this type of attenuation with present timber measurements is lacking, a test to check any theory is unavailable. However, by the nature and distribution of signal strengths from the mountaintop tests, the following theoretical attenuation model is contemplated for the tree crowns:

$$\phi_x = \phi_0 e^{-\delta x}$$

where δ is related to crown characteristics and x is the optical path length, i.e.:

$$x = \frac{h}{\operatorname{Cos} \theta}$$

where h = crown depth, and θ = aspect angle as before. Further field measurements should provide data for correlation checks on these proposed relations.

The ultimate objective of these considerations is to provide field management personnel with a measure of the usefulness of remote sensing equipment in particular forested areas.

Security Classification

DOCUMENT CONTROL DATA - R&D

(Security classification of title, body of abstract and indexing annotation must be entered when the overall report is classified)

1. ORIGINATING ACTIVITY (Corporate author)
U.S. Department of Agriculture, Forest Service
Intermountain Forest & Range Exp. Sta.
Northern Forest Fire Laboratory, Missoula, Montana

2a. REPORT SECURITY CLASSIFICATION
Unclassified

2b. GROUP

3. REPORT TITLE
Project Fire Scan Fire Detection Interim Report

4. DESCRIPTIVE NOTES (Type of report and inclusive dates)
Interim Report, April 1962 to December 1964

5. AUTHOR(S) (Last name, first name, initial)
Wilson, Ralph A.
Noste, Nonan V.

6. REPORT DATE
June 1966

7a. TOTAL NO. OF PAGES
68

7b. NO. OF REFS
12

8a. CONTRACT OR GRANT NO.
OCD-OS-62-174
ARPA ORDER #636

b. PROJECT NO.
WORK UNIT 2521A

c.

d. ARPA PROGRAM CODE NO. 3860

9a. ORIGINATOR'S REPORT NUMBER(S)
RESEARCH PAPER INT-28, 1966

9b. OTHER REPORT NO(S) (Any other numbers that may be assigned this report)

10. AVAILABILITY/LIMITATION NOTICES
DISTRIBUTION OF THIS DOCUMENT IS UNLIMITED.

11. SUPPLEMENTARY NOTES STUDY TITLE:
"THE EVALUATION OF AN AIRBORNE INFRARED MAPPER AS A TOOL FOR DETECTING AND MEASURING FIRES."

12. SPONSORING MILITARY ACTIVITY
DEPARTMENT OF THE ARMY
OFFICE OF THE SECRETARY OF THE ARMY
OFFICE OF CIVIL DEFENSE
WASHINGTON, D. C. 20310

13. ABSTRACT
The first 3 years of Project Fire Scan's airborne infrared fire detection program are reported. The program objective is the evaluation of systems and techniques for the detection of incipient forest fires. Qualitative correlations are presented of probability of detection versus scanner aspect angle, timber type, and fire target size. Aircraft patrol navigation requirements are briefly examined. A capability is demonstrated for precise observations of timber canopy obscurations from a fixed, ground platform. Appendixes include theoretical discussions of system spectral response, scanner sensitivity, source background radiometric detection criteria, and the several mechanisms of radiation attenuation.

FORM AN 64 1473

Security Classification

KEY WORDS	LINK A ROLE	LINK A WT	LINK B ROLE	LINK B WT	LINK C ROLE	LINK C WT
airborne infrared fire detection						
evaluation of systems and techniques for the detection of incipient forest fires						
probability of detection						
scanner aspect angle						
timber type						
fire target size						
patrol navigation requirements						
timber canopy obscurations						
fixed, ground platform						
system spectral response						
scanner sensitivity						
radiometric detection criteria						
mechanisms of radiation attenuation						

INSTRUCTIONS

1. ORIGINATING ACTIVITY: Enter the name and address of the contractor, subcontractor, grantee, Department of Defense activity or other organization *(corporate author)* issuing the report.

2a. REPORT SECURITY CLASSIFICATION: Enter the overall security classification of the report. Indicate whether "Restricted Data" is included. Marking is to be in accordance with appropriate security regulations.

2b. GROUP: Automatic downgrading is specified in DoD Directive 5200.10 and Armed Forces Industrial Manual. Enter the group number. Also, when applicable, show that optional markings have been used for Group 3 and Group 4 as authorized.

3. REPORT TITLE: Enter the complete report title in all capital letters. Titles in all cases should be unclassified. If a meaningful title cannot be selected without classification, show title classification in all capitals in parenthesis immediately following the title.

4. DESCRIPTIVE NOTES: If appropriate, enter the type of report, e.g., interim, progress, summary, annual, or final. Give the inclusive dates when a specific reporting period is covered.

5. AUTHOR(S): Enter the name(s) of author(s) as shown on or in the report. Enter last name, first name, middle initial. If military, show rank and branch of service. The name of the principal author is an absolute minimum requirement.

6. REPORT DATE: Enter the date of the report as day, month, year; or month, year. If more than one date appears on the report, use date of publication.

7a. TOTAL NUMBER OF PAGES: The total page count should follow normal pagination procedures, i.e., enter the number of pages containing information.

7b. NUMBER OF REFERENCES: Enter the total number of references cited in the report.

8a. CONTRACT OR GRANT NUMBER: If appropriate, enter the applicable number of the contract or grant under which the report was written.

8b, 8c, & 8d. PROJECT NUMBER: Enter the appropriate military department identification, such as project number, subproject number, system numbers, task number, etc.

9a. ORIGINATOR'S REPORT NUMBER(S): Enter the official report number by which the document will be identified and controlled by the originating activity. This number must be unique to this report.

9b. OTHER REPORT NUMBER(S): If the report has been assigned any other report numbers *(either by the originator or by the sponsor)*, also enter this number(s).

10. AVAILABILITY/LIMITATION NOTICES: Enter any limitations on further dissemination of the report, other than those imposed by security classification, using standard statements such as:

(1) "Qualified requesters may obtain copies of this report from DDC."

(2) "Foreign announcement and dissemination of this report by DDC is not authorized."

(3) "U. S. Government agencies may obtain copies of this report directly from DDC. Other qualified DDC users shall request through _____."

(4) "U. S. military agencies may obtain copies of this report directly from DDC. Other qualified users shall request through _____."

(5) "All distribution of this report is controlled. Qualified DDC users shall request through _____."

If the report has been furnished to the Office of Technical Services, Department of Commerce, for sale to the public, indicate this fact and enter the price, if known.

11. SUPPLEMENTARY NOTES: Use for additional explanatory notes.

12. SPONSORING MILITARY ACTIVITY: Enter the name of the departmental project office or laboratory sponsoring *(paying for)* the research and development. Include address.

13. ABSTRACT: Enter an abstract giving a brief and factual summary of the document indicative of the report, even though it may also appear elsewhere in the body of the technical report. If additional space is required, a continuation sheet shall be attached.

It is highly desirable that the abstract of classified reports be unclassified. Each paragraph of the abstract shall end with an indication of the military security classification of the information in the paragraph, represented as *(TS)*, *(S)*, *(C)*, or *(U)*.

There is no limitation on the length of the abstract. However, the suggested length is from 150 to 225 words.

14. KEY WORDS: Key words are technically meaningful terms or short phrases that characterize a report and may be used as index entries for cataloging the report. Key words must be selected so that no security classification is required. Identifiers, such as equipment model designation, trade name, military project code name, geographic location, may be used as key words but will be followed by an indication of technical context. The assignment of links, rules, and weights is optional.